NEXT-C Flight Ion System Status

Jack Fisher¹, Brian Ferraiuolo², Jeff Monheiser³, Keith Goodfellow⁴, Andy Hoskins⁵ and Roger Myers⁶

Aerojet Rocketdyne, Redmond WA, United States

Jim Bontempo⁷, Jim McDade⁸
ZIN Technologies, Cleveland OH, United States

Terry O'Malley⁹, George Soulas¹⁰, Rohit Shastry¹¹ and Marcelo Gonzalez¹²

NASA Glenn Research Center, Cleveland, OH, United States

The 7.4 kW NEXT-C (NASA's Evolutionary Xenon Thruster – Commercial) gridded ion thruster system provides a combination of performance and spacecraft integration capabilities that make it uniquely suited for deep space robotic missions. With modifications, the NEXT-C system can meet some high total impulse defense and commercial missions as well. The purpose of the NEXT-C flight hardware development program, jointly funded by NASA and Aerojet Rocketdyne, was to establish a commercial supply of the thruster and power processing unit (PPU) for future NASA missions. The program has completed all development and flight production testing and delivered the first shipset of flight hardware to NASA GRC in early 2020 for use on the Applied Physics Laboratory's DART (Double Asteroid Redirection Test) mission. The NEXT system was developed to a readiness approaching TRL 6 in the mid-2000s, followed by characterization and long duration testing at NASA Glenn Research Center. The original NEXT project effort culminated in a long duration life test of 50,000 hours on a NASA EM thruster using Aerojet Rocketdyne high fidelity optics. The thruster is throttleable across a thrust range of approximately 25 to 235mN. Thruster specific impulse ranges from 1400 to 4200sec, depending on the throttle condition. Each NEXT-C thruster is powered by a PPU with an input power of up to 7.4kW. The PPU converts spacecraft power, over an unregulated input voltage range from 80 to 160 volts, to the conditions required to operate the thruster, and also utilizes spacecraft 28 Volt power to operate the PPU's communication and control circuitry. On the NEXT-C program, the component designs have matured to include design updates to increase capability, address issues identified during the development program, and incorporate lessons learned. Aerojet Rocketdyne has completed all program phases of the project, including full protoflight and integration testing of the Engineering Model hardware, Critical Design Review, ground test equipment validation, fabrication of flight hardware and protoflight level acceptance testing. Flight hardware testing included both component level testing of the flight PPU and thruster, culminating in an integrated system level hot fire test that demonstrated the flight controls and operating parameters planned to be utilized on the DART mission. The flight hardware testing was successfully completed to the DART mission requirements. This paper will present the flight system capabilities, latest test results, and flight hardware status for the NEXT-C ion engine system.

¹ NEXT-C Program Manager, Jack.Fisher@rocket.com.

² NEXT-C Chief Engineer, Brian.Ferraiuolo@rocket.com.

³ NEXT-C Subject Matter Expert, Jeff.Monheiser@rocket.com.

⁴ NEXT-C Chief Engineer, Keith.Goodfellow@rocket.com.

⁵ NEXT-C Technical Consultant, William. Hoskins@rocket.com.

⁶ NEXT-C Technical Consultant, Roger.Myers@rocket.com.

⁷ ZIN Technologies Electrical Lead, bontempoj@zin-tech.com.

^{8 7}IN Taskas lasis Durana Managar Malalai@in task and

⁸ ZIN Technologies Program Manager, Mcdadej@zin-tech.com.

⁹ NASA Project Manager, tfomalley@nasa.gov

¹⁰ NASA Product Lead Engineer, Rohit.Shastry@nasa.gov.

¹¹ NASA Thruster Lead, George.C.Soulas@nasa.gov.

¹² NASA PPU Lead, Marcelo.C.Gonzalez@nasa.gov.

I. Nomenclature

APL = Applied Physics Laboratory AR = Aerojet Rocketdyne CDR = Critical Design Review

DART = Double Asteroid Redirection Test
DCIU = Digital Control Interface Unit

EEE = Electrical, Electronic and Electromechanical

EP = Electric Propulsion EM = Engineering Model

EMC = Electromagnetic Compatibility EMI = Electromagnetic Interference

FT = Flight Thruster
GEO = Geosynchronous
GRC = Glenn Research Center
GSE = Ground Support Equipment
HAR = Hardware Assurance Review
JPL = Jet Propulsion Laboratory
LDT = Long Duration Test

NEXT = NASA's Evolutionary Xenon Thruster

NEXT-C = NASA's Evolutionary Xenon Thruster – Commercial

NSTAR = NASA Solar Electric Propulsion Technology Applications Readiness

PDR = Preliminary Design Review
PM1R = Prototype Model #1 Revised
PMS = Propellant Management System

PPU = Power Processing Unit SEP = Solar Electric Propulsion SIT = System Integration Test TRL = Technology Readiness Level

TVAC = Thermal Vacuum VF = Vacuum Facility

II. Introduction

The 7.4kW NEXT-C (NASA's Evolutionary Xenon Thruster – Commercial) gridded ion thruster system, shown in Figure 1, provides a combination of performance and spacecraft integration capabilities that make it uniquely suited for deep space robotic missions, as well as some GEO missions. The gridded ion thruster remains the highest performance (specific impulse) electric propulsion technology in use, especially suited for ambitious, high ΔV missions requiring high specific impulse and long life. The NEXT-C system can independently control power and flow parameters enabling throttling by an order of magnitude in thrust and required input power, which is critical for solar powered missions traveling large distances from the sun. Additionally, the relatively simple acceleration physics of the gridded ion engine allows for excellent correlation between ground test and in space performance. Finally, the highly collimated beam allows greater flexibility in locating the thruster on the spacecraft while avoiding impingement of the exhaust on spacecraft surfaces, reducing communications impacts, and allowing a reduction of the off-axis pointing and associated thrust loss for geosynchronous (GEO) satellite orbit-raising.

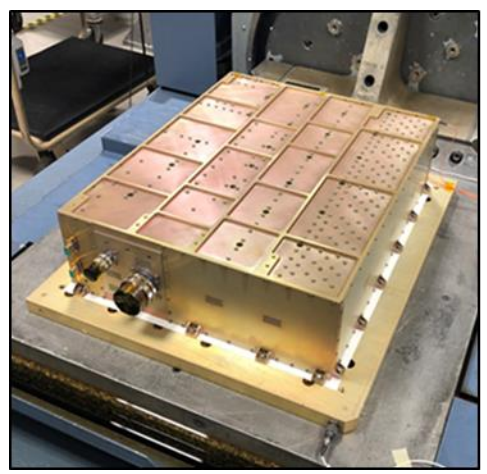




Fig. 1 NEXT-C Flight PPU and Thruster.

Challenging NASA science missions that would greatly benefit or be enabled by the NEXT-C system include, small body mission studies, such as Comet Surface Sample Return, outer planet, deep space telescope, and Mars sample return type vehicles. In addition to the NASA missions, national security space missions with very high ΔV requirements have been identified as potential applications for NEXT-C systems. Finally, the use of NEXT-C systems on Comsats for GEO orbit acquisition is under continued investigation. Challenges include reducing the recurring cost of the flight hardware without sacrificing extensive life test heritage, increasing the thrust/power ratio to reduce transit times, and providing a closer to "drop-in replacement" physical configuration at the gimbal footprint.

The near term application for the NEXT-C system is NASA's Double Asteroid Redirection Test (DART) mission, which will demonstrate a single NEXT-C thruster and PPU propulsion system. Launching in mid-2021, this mission involves impacting the smaller of a co-orbiting binary asteroid, Dimorphos, in October 2022 with a >300 kg spacecraft. The goal is to demonstrate and characterize the deflection of a hazardous asteroid with the momentum transfer from a very high speed impact by the spacecraft. By impacting the smaller, 150m asteroid and monitoring the change in its orbit around the 800m partner, it will be possible to characterize the deflection much more precisely than to detect the change in the heliocentric orbit of a single asteroid. The flight Thruster and PPU planned for use on this mission have successfully completed both component and system level testing and have been delivered to APL for integration onto the spacecraft.



Fig. 2 DART Spacecraft Approaching Dimorphos.

III. NEXT Ion System Background

From the success of 2.5kW NSTAR system on the Deep Space-1 mission⁵, NASA studies in 2001 showed that development of a higher power ion engine was enabling for many of NASA's future planetary science missions. In 2002, NASA's Science Mission Directorate awarded NASA's Evolutionary Xenon Thruster (NEXT) program under the In-Space Propulsion Technology project to a team led by NASA Glenn Research Center (GRC). The goal of the program was to develop a 7 kW class Ion Propulsion System, including thruster, Power Processing Unit (PPU), Propellant Management System (PMS), Digital Control Interface Unit (DCIU) and gimbal. The team included JPL, which was responsible for some of the testing and analysis and the gimbal development; L-3 Communications, which was responsible for PPU development; and Aerojet Rocketdyne (AR), which was responsible for thruster, PMS and DCIU development. ^{6,7}

AR significantly upgraded the NASA Engineering Model (EM) thruster design to a more robust, flight weight EM design, dubbed the "Prototype Model" or "PM" thruster. Following delivery of hardware by L-3 and AR in 2006, NASA GRC and JPL conducted comprehensive testing, both as individual components and as integrated combinations, of the NEXT ion propulsion system. These included detailed performance characterization, vibration, and thermal vacuum testing at qualification levels, as well as a 2,000 hour test of the thruster. Table 1 Table 1 gives a partial performance table for the thruster/PPU system. Additionally, NASA GRC conducted a Long Duration Test (LDT) of a GRC-built EM thruster with AR-built PM design optics that was operated a record breaking 50,000 hours and consumed 900 kg of Xe. 89,12 The total impulse of 35 MN-s is over three times the total impulse demonstrated on any other electric propulsion thruster. Under the program the L-3 Engineering Model (EM) PPU achieved Technology Readiness Level (TRL) 4. The AR "PM" thruster and EM PMS both achieved TRL 6 by the end of the NEXT program. 10

Beam Voltage V	Beam Current A	PPU Input Power kW	Thruster Efficiency	Thrust mN	Specific Impulse s	Thrust / Power mN/kW
1800	3.52	7.33	0.70	235	4155	32
1800	2.70	5.65	0.68	178	4082	32
1800	1.20	2.61	0.61	78	3882	30
1396	3.52	5.84	0.69	208	3683	36
1396	2.70	4.51	0.67	159	3626	35
1396	1.20	2.15	0.59	69	3432	32
1021*	2.70	3.48	0.66	137	3137	39
1021	1.20	1.70	0.57	59	2953	35
679	2.70	2.55	0.60	111	2565	43
275	1.00	0.64	0.32	25	1395	39

Table 1. Selected NEXT-C Throttle Points.

IV. NEXT-C Program Overview

While there was interest in the NEXT system for multiple NASA science programs, a barrier to infusion was the cost and risk of completing development, qualifying the system, and building the first flight units, all of which would have been borne by the first mission. In order to facilitate the incorporation for use in NASA missions, NASA decided initiate the NEXT-C program in 2015.

The program is focused only on the thruster and PPU because those are the key components specific to the NEXT system. Needs and approaches to the DCIU, propellant feed system and gimbal may be more mission specific, and other component options with flight heritage may already exist. The overall approach of the development phase of the NEXT-C program was to address known issues with the current PPU and thruster designs, meet any updates to

^{*} Throttle point to be used by DART¹¹

the requirements, and make design changes that would reduce cost while maintaining the validity of the testing to date, in particular the 50,000 hr long duration test, which would not be feasible to repeat.

The NEXT-C program was awarded to Aerojet Rocketdyne in March of 2015 with the goal of completing flight system development and delivery of two sets of flight PPUs and thrusters. There has been close collaboration with NASA GRC and the industry NEXT-C team, comprised of Aerojet Rocketdyne, who is responsible for system integration, thruster development and manufacture, and PPU development oversight, and AR's subcontractor, ZIN Technologies, who is responsible for PPU development and manufacture. The NEXT-C overall program objectives were to mature the thruster and PPU elements from the NEXT Program from TRL 4 (PPU)/TRL 6 (thruster) to TRL 8.¹⁷ The program was to provide two flight fidelity thrusters and PPUs for use on a future NASA science missions.

The NEXT-C program included the following key elements:

- System Requirements development and flow down to individual components
- Detailed Design and Analyses of both the Thruster and PPU, suitable for prototype hardware fabrications
- Manufacture of a flight like prototype PPU and development thruster
- Development testing at qualification and protoflight levels for the PPU, Thruster, and combined System Integration Testing (SIT)
- Formal PDR, CDR and HAR review meetings
- Release of Production/Flight level drawings for both the PPU and thruster
- Production Tooling to support flight hardware build
- Manufacture of two sets of Flight PPUs and Thrusters
- Development of GSE to support flight acceptance testing of the PPU, thruster and system level integration testing
- Protoflight level acceptance testing of PPU, thruster and system level integration testing.

The program progressed through the various development and flight manufacturing phases from 2015 through 2020, as shown in Figure 2 below. In 2019 there were two significant programmatic modifications implemented to the original program plan. Given that the first set of flight hardware was designated to support the DART mission, the acceptance testing was modified to more closely model the DART mission operating parameters, as described in subsequent sections. In addition, due to funding limitations, in late 2019 the final assembly and testing of the 2nd set of flight hardware was suspended. A complete set of piece parts and most subassemblies were completed prior to this action being implemented and are being maintained for a future contract.

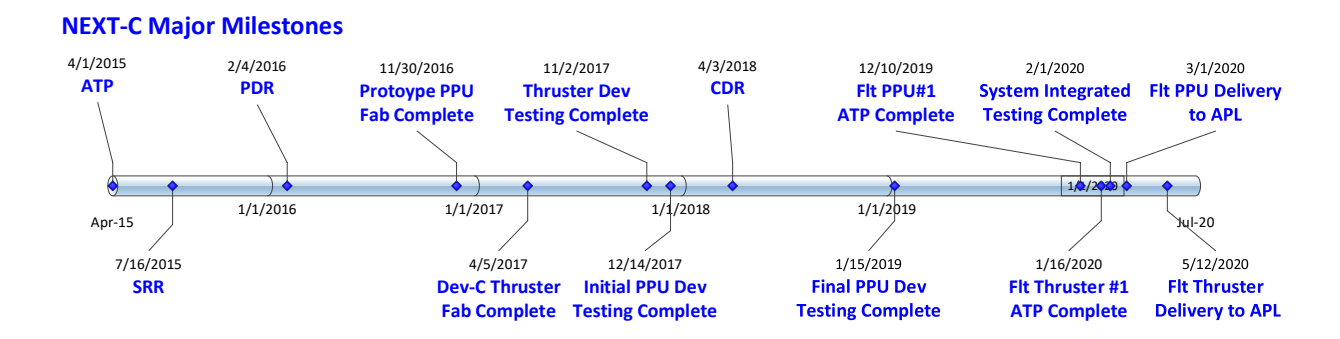


Fig. 3 NEXT-C Program Timeline from Award to Flight Hardware Delivery.

This paper summarizes the status of the NEXT-C program, including summaries of both development and flight hardware testing performed with the thruster and power processor, as well as the results of integrated system testing.

V. NEXT-C Thruster Design Overview

NEXT-C is a gridded Ion Engine that is designed to run on xenon propellant. Its design lineage dates back to the 2.5 kW NSTAR System. Initial work at NASA GRC from 2001 to 2003 on a larger engine scaled to operate at up to 7 kW resulted in Engineering Model design that was the starting point of the NEXT program. AR's flight-weight Prototype Model thruster from the original NEXT program served as the starting point for the NEXT-C program.^{8,9} For the NEXT-C program, the design of propellant wetted surfaces, which dictate thruster performance and life, were not changed in order to ensure heritage to the extensive testing and performance that has been previously demonstrated by NASA. The NEXT-C thruster design implements some updates for manufacturability and for increased structural capability to survive launch loads and mechanism deployments.

NEXT-C is a two grid, ring-cusp thruster. However, in contrast to the NSTAR thruster, NEXT-C produced a slightly larger, 36 cm diameter, ion beam with a more uniform beam current density. The highest and lowest operating points listed in Table 1 show that the NEXT-C thruster has an almost 10 to 1 throttle range (235:25 mN) which increases the applicability of the thruster to future NASA near-Earth and planetary missions.

The thruster is comprised of four major subassemblies, as shown in Fig. 4 & 5,: the Ion Optics (often referred to as "grids" or "electrodes"), the Discharge Chamber Assembly, the Discharge Cathode Assembly, and the Neutralizer Cathode Assembly. Its envelope is roughly 25" in diameter by 17" in total height and weighs approximately 14kg. It mounts to the spacecraft structure, or gimbal, by 3 mounts each with 4 locking nutplates. The thruster interfaces electrically via two harnesses (one for discharge and the other for the neutralizer) and interfaces with the propellant feed system via three 1/8" tube interfaces. The thruster harnesses are 2 meters long in standard configuration, and have been system tested with longer harnesses to extend to the distance between the thruster and PPU location on the spacecraft. The propellant interfaces can be configured to be a welded configuration or a number of threaded interfaces/fittings.

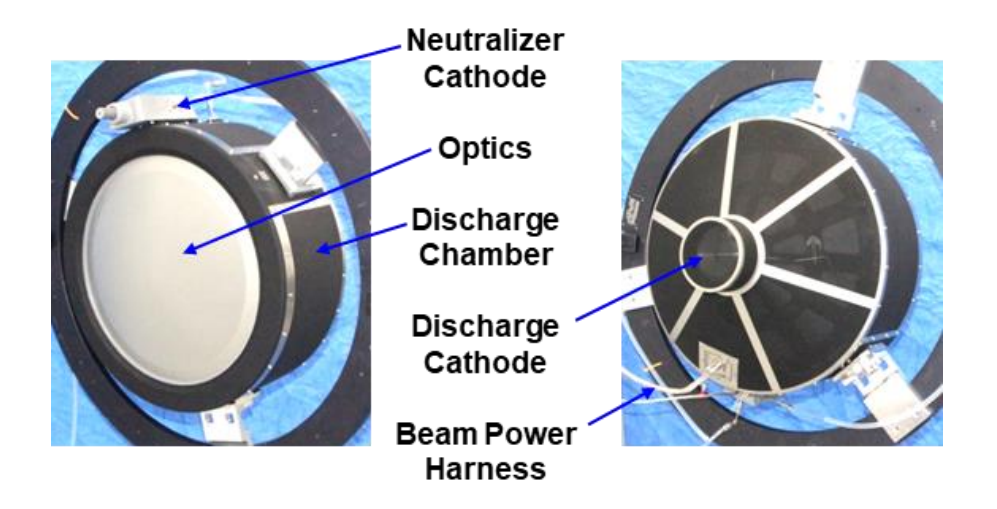


Fig. 4 NEXT-C Thruster Major Subassemblies.

The basic operation is similar to any other gridded ion engine. The discharge cathode is a hollow cathode, which emits electrons into the discharge chamber. Xenon propellant is fed into the discharge chamber where the xenon atoms are impacted by the electrons to create ions. The discharge chamber houses rings of permanent magnets to limit electron losses and maximize the ion creating collisions. The optics, or grids, then accelerate the ions through the thousands of apertures using a high voltage potential between the two grids, creating thrust. Finally, a second hollow cathode, the neutralizer cathode, which is outside of the discharge chamber, also creates electrons which create a bridge for the neutralization current for the plume.

Design updates implemented on the NEXT-C program resulted in a gridded ion thruster that is more structurally capable and has improved manufacturability and spacecraft integration than earlier versions. The total throughput and life capability of the NEXT-C thruster has been validated by a combination of long duration tests and analysis. The primary test data comes from the previously noted 50,000 hour lifetest that had an optics assembly built by AR and of identical design to the flight optics assembly. By maintaining the materials and dimensions of all other "plasma-wetted" surfaces, the life assessment of the flight design can rely on the long duration test results, bolstered by analysis. Over a dozen known gridded ion engine wear out mechanisms have been evaluated for NEXT-C in a probabilistic life assessment.¹³ The life limiting mechanism at low power levels was found to be screen grid erosion, with TL5 being the worst case, and at high powers, electron backstreaming due to accelerator grid hole wall erosion, with TL40 being the worst case. 14 While a more refined life estimate requires consideration of the specific profile of throttle levels planned for a mission, a worst case minimum of 700 kg xenon can be run through the thruster at TL40 over 34,500 hours before the electron backstreaming limit is met at standard accel grid voltages. Analysis results indicate that operation could be extended beyond this point at least another 200 kg by adjusting the accel voltage more negatively by only 5-10% during the mission. Therefore, 700 kg represents a conservative minimum throughput, and it may be possible to validate considerably more throughput capability depending on the details of the mission assumptions.



Fig. 5 NEXT-C Flight Thruster in Final Assembly at AR.

VI. NEXT-C PPU Design Overview

The PPU design is baselined from the previous test bed developed on the NEXT program, which has successfully operated the NASA ion thrusters. The NEXT-C PPU has incorporated lessons learned from the previous testing as well as incorporated solutions to issues uncovered from more recent development testing. Additionally, electrical components have been upgraded to take advantage of current technology where applicable and to address obsolescence.

The NEXT-C Power Processing Unit (PPU) provides the electrical power to the thruster and reports the telemetry of the thruster system. The PPU powers a 7kW class gridded-ion thruster as shown in Figures 6, 7 and Table 2, consisting of:

- Beam Supply (~85% Total Power)
 - Positive Grid Electrostatic Field with regulated voltage up to 1,800V
- Discharge Supply (~10% Power)
 - Ionizes Xenon and is current regulated
- Quad Supply (~5% Total Power)
 - Accelerator (Negative) Grid, Neutralizer, Discharge and Neutralizer Heaters
- Communicates via an RS-485 serial link
 - Command and Telemetry is configurable; fully redundant A and B channels or can send on channel A and receive on channel B for compatibility with older equipment.

The PPU weighs less than 35kg and is conductively cooled through the base plate. At base plate temperatures between -29°C to 55°C, PPU efficiencies exceed the design requirements with over 90% efficiency at most power levels. At full output power, the PPU efficiency is up to 95%. It communicates via an RS-485 serial link that is configurable; fully redundant A and B channels or can send on channel A and receive on channel B for compatibility with older equipment.

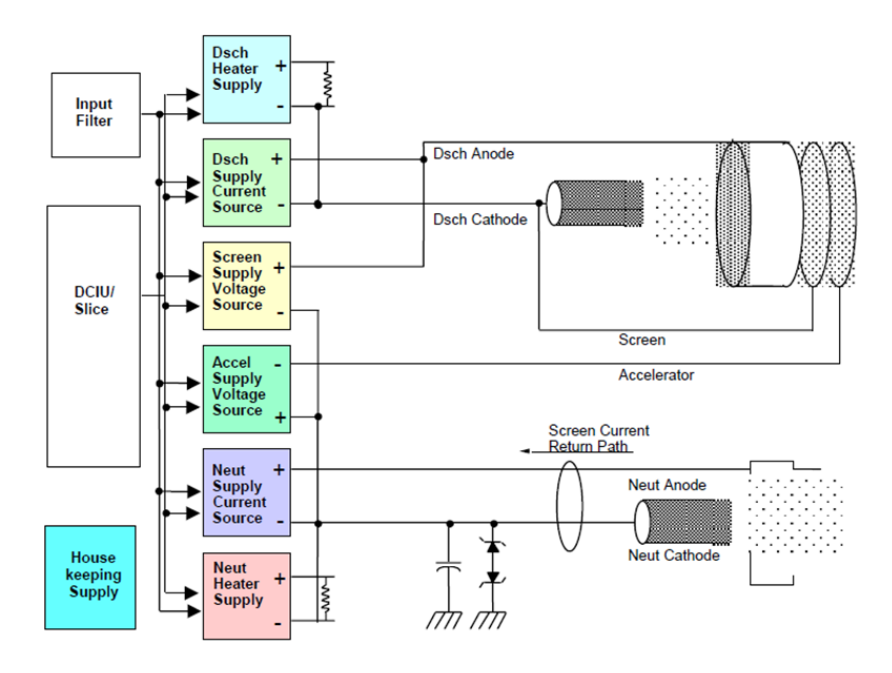


Fig. 6 Electrical Block Diagram of NEXT-C System.

Table 2. NEXT-C PPU Output Power Characteristics

	Neutralizer		Neutralizer Heater		Discharge		Discharge Heater		Screen		Accel	
Input Voltage		80 to 160 Volt DC High Power Bus, 22 to 34 Volt DC Low Power Bus										
Output Voltage (VDC)	8	32	3	12	15	35	3	24	275	1800	115	525
Output Current (ADC)	1	3	3.5	8.5	4	24	3.5	8.5	1	3.52	0	0.04
Regulation	Current- Controlled		Current- Controlled		Current- Controlled		Current- Controlled		Voltage- Controlled		Voltage- Controlled	
Setpoint Accuracy (% of Setpoint Value)	2.5%		2.5%		2.5%		2.5%		2.5%		2.5%	
Output Ripple (% of Setpoint Value)	51	5%		5%		5%		5%		5%		%
Max Power Out (W)	96		102		840		204		63	36	2	21
Minimum Efficiency (%) at Max Power Out @ TL40 (W)	> 93.5% (a) /360 W											

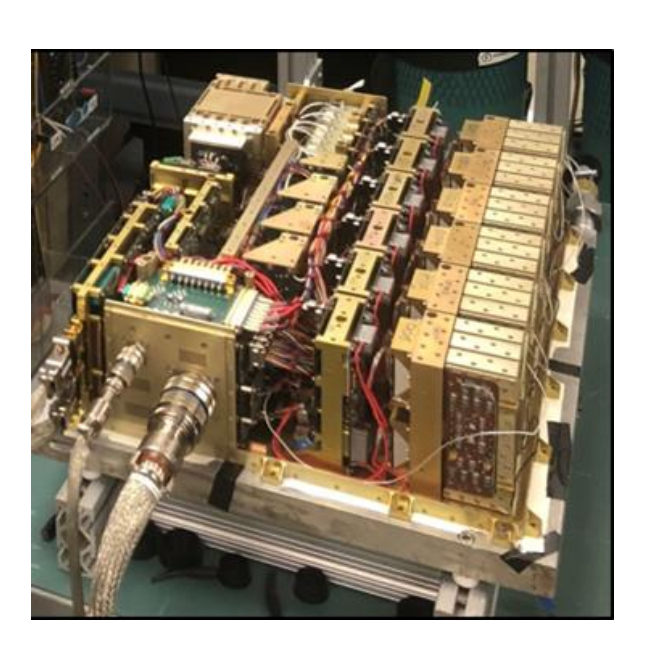


Fig. 7 NEXT-C Flight Power Processing Unit (cover off).

VII. Development Hardware Testing

Both the prototype thruster and PPU completed extensive development testing to verify operation of each component as well as mitigate risk of anomalies during testing of the flight hardware. This included multiple integrated system tests, including ones that direct simulated the mission operating parameters for the DART mission.

As mentioned previously, the thruster design is based on heritage designs with the intent to maintain commonality for all propellant wetted surfaces thereby ensuring that previous long duration tests are still valid. One of the key program goals for NEXT-C was to upgrade the previous prototype design to incorporate lessons learned from the initial manufacturing, as well as from previous flight programs and finally to make the design more commercially viable. As such, the prototype model thruster, PM1R, was retrofitted to incorporate those changes that we deemed to be slightly risky to the thruster performance and ability to survive environmental testing. This new version of the prototype thruster was dubbed "DEV-C". These retrofits included harness upgrades, mounting flange upgrades for both cathodes, and an upgrade to the neutralizer enclosure to aid in the final assembly. The thruster then underwent development testing to ensure that the changes did not affect the capabilities of the thruster. This development testing was completed in 2018 and included early integrated system testing, random vibration, qualification level shock and post-structural performance testing as shown in Fig. 8.

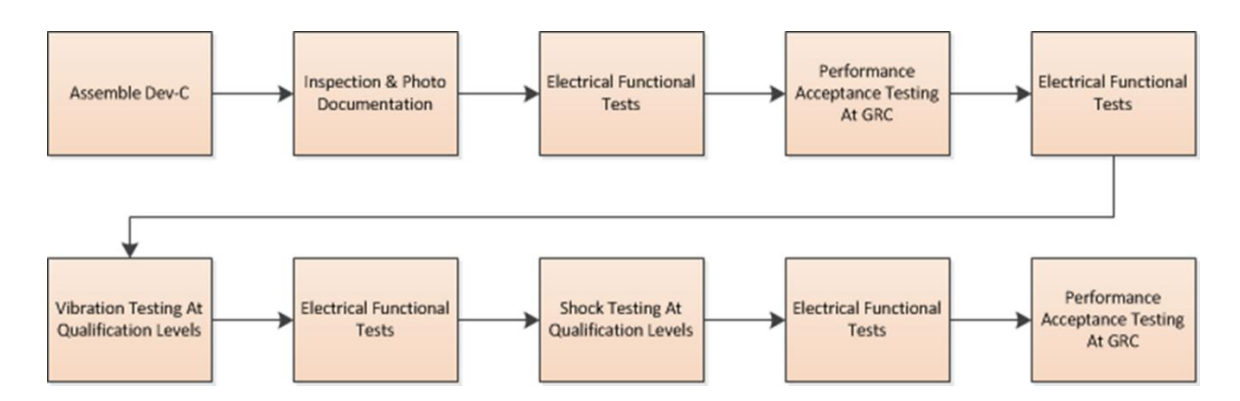


Fig. 8 DEV-C Thruster Test Campaign.

The vibration testing of the thruster was performed at NASA Glenn Research Center and was completed for all three axis. The thruster was tested without a gimbal, and as such, interface environments were derived and a force limiting test method was applied. Testing the development thruster served to both verify the operation of the test equipment, the fixture and table controls, as well as verified that the changes applied to the thruster did not affect its vibration characteristics or natural frequencies. It also confirmed the structural improvements made to the design were valid. The test was a protoflight test, meaning it was qualification level environments for acceptance duration (60 seconds per axis). Sine sweeps were performed before and after each axis to ensure no shifts in natural frequency responses that would be indicative of a hardware issue. The vibration test was a success and no hardware or performance degradation of the thruster was noted. Figure 9 shows the DEV-C thruster mounted on the vibration table at NASA GRC and for this particular picture, the thruster is begin tested in the Y axis.

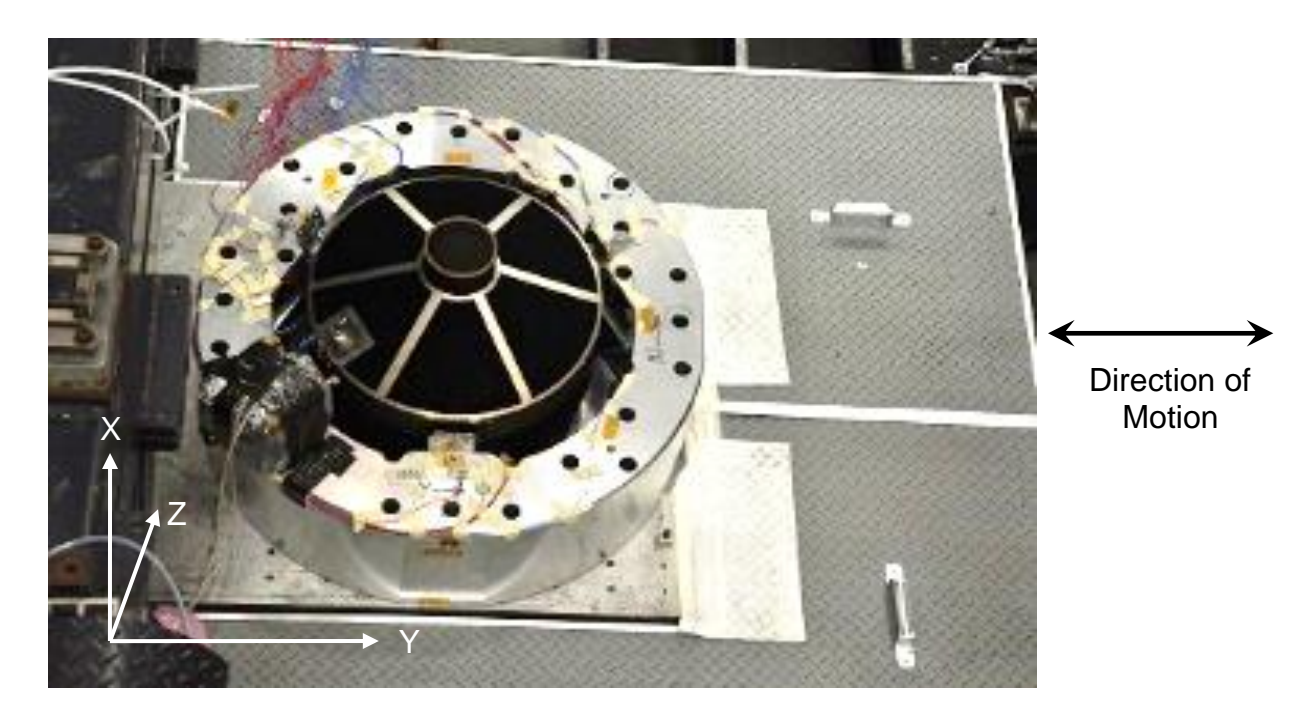


Fig. 9 DEV-C thruster mounted on the vibration table (Y axis).

As mentioned, one of the objectives for this development testing was to verify that the experimental setup was capable of conducting the test without harming the thruster. This testing demonstrated the control system was capable of controlling the input frequency spectrum and limiting the applied force levels. Based on this, it was decided by the program that the test methodology was ready for testing of the flight thruster.

Once the vibration testing was competed, the thruster was shipped to an external vendor for qualification shock testing. As the program plan was to perform protoflight testing on each flight unit, a dedicated qualification test unit was not planned. For shock verification, it is atypical to perform shock testing on flight hardware in excess of planned flight loads. Therefore, the formal qualification verification shock test was performed on the prototype Dev-C thruster. In addition to the testing itself, there was an extensive differences assessment made between the Dev-C thruster design and the flight design to ensure the shock test was representative and could be used to verify qualification requirements. Because this is a qualification test, the thruster was subjected to two shock loads in each direction using the setup shown in Fig. 10. Multiple test runs were completed in each axis with a mass simulator to first tune the system and test responses prior to testing the thruster.

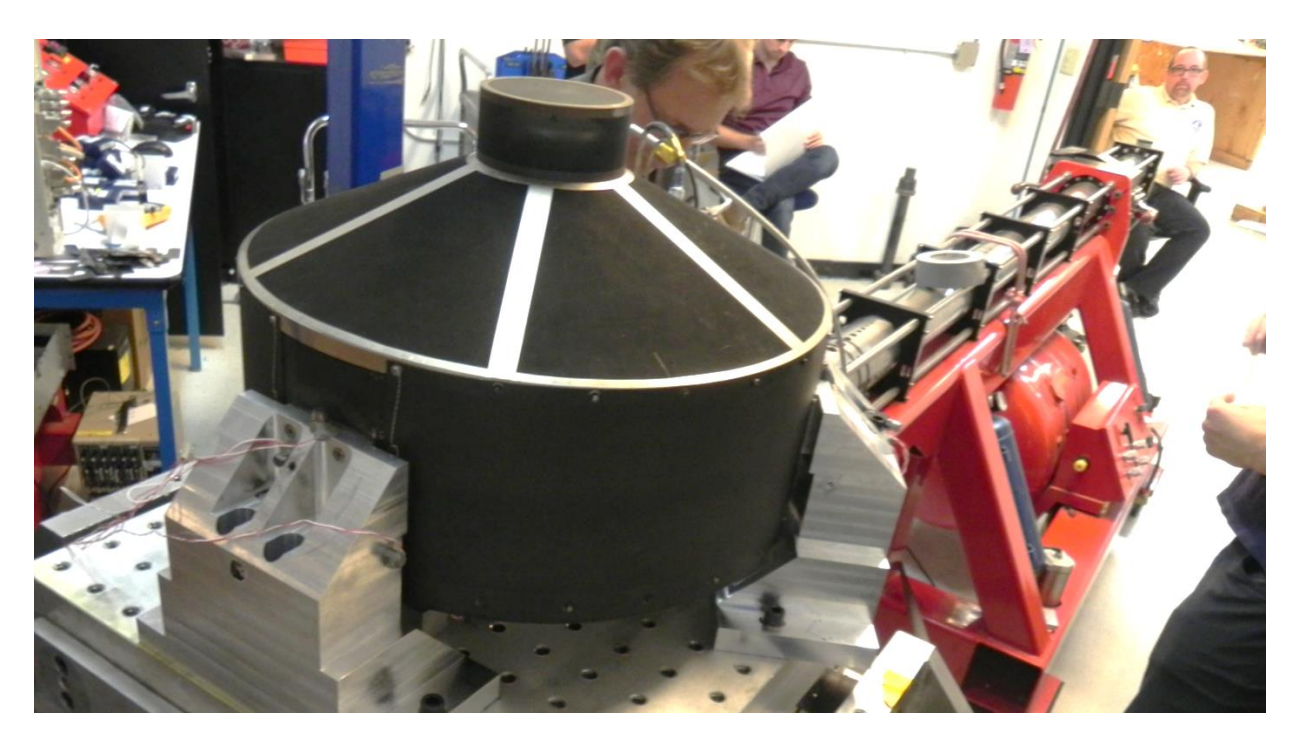


Fig. 10 DEV-C Thruster Undergoing Shock Testing.

After shock testing was performed, the thruster was inspected for any damage. Notably, the ceramic hardware within the thruster was inspected for any signs of damage and or cracking and none was observed. The thruster then underwent a post-environmental hot fire test to confirm there were no shifts in its performance. Figures 11 and 12 are a comparison of the discharge chamber performance and electron backstreaming data obtained both prior to and post environmental testing. Reviewing the data shows no observable shifts in performance before or after environmental testing. It should be noted that these two parameters were chosen because they are the most sensitive to changes in the thruster operation. Based on this testing, it was concluded that the changes proposed to be implemented in the flight thruster design were very low risk.

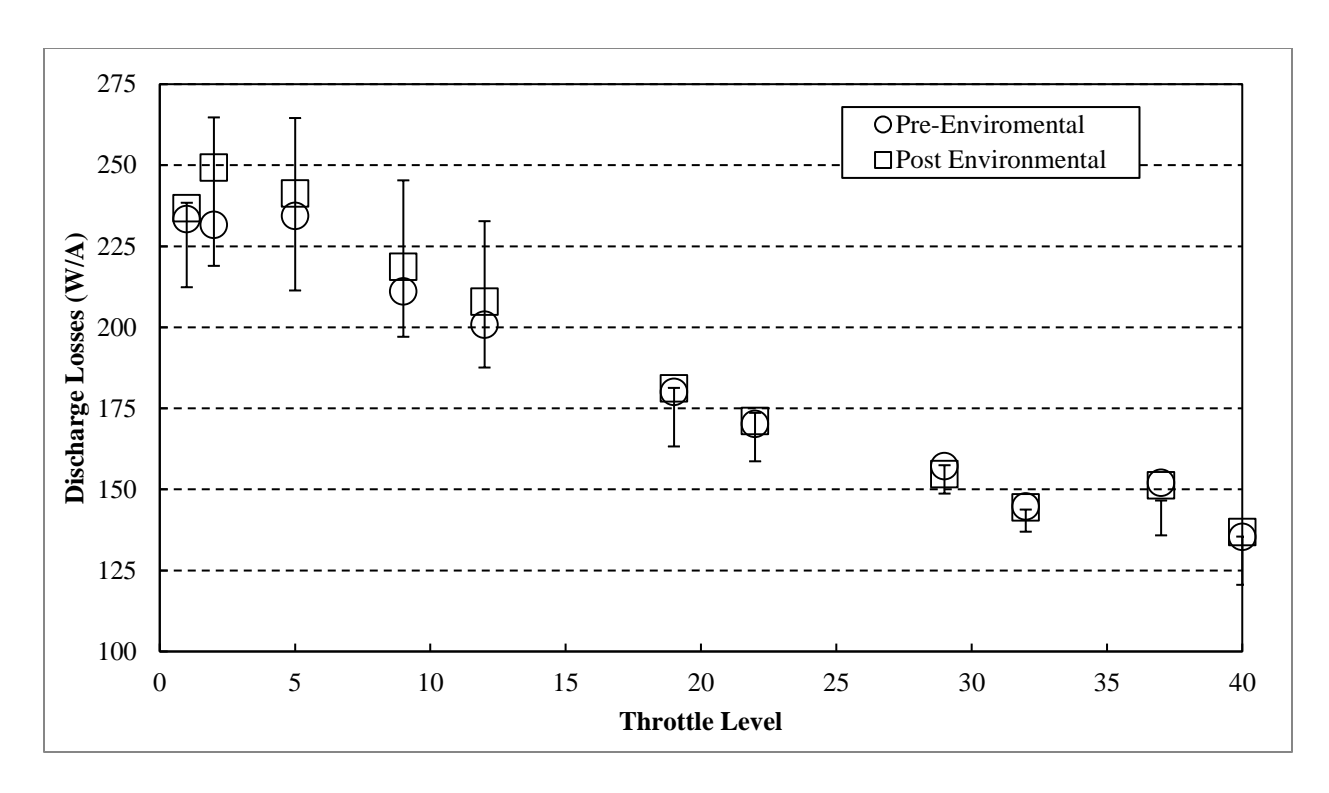


Fig. 11 Discharge Chamber Performance – Pre and Post Environmental Testing

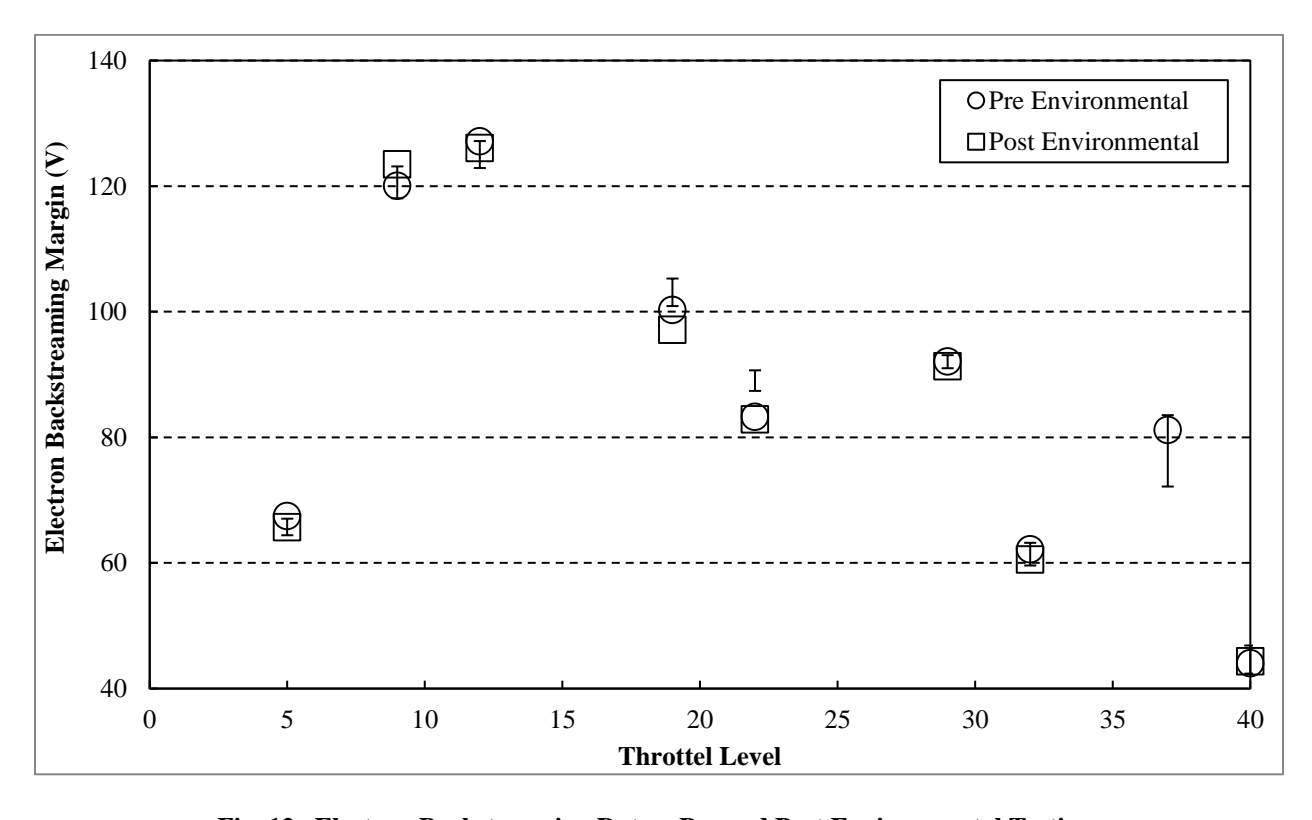


Fig. 12 Electron Backstreaming Data – Pre and Post Environmental Testing.

The prototype PPU completed two series of environmental tests including EMI/EMC, mechanical shock, vibration and thermal-vacuum testing. As expected, during the first round of PPU development testing performed in 2017 multiple issues were identified as the PPU was initially operated over it full operating range and environment. Each issue was carefully assessed, mitigated and its solution was demonstrated during subsequent repeat testing. Upon completion of the design upgrades made to the prototype PPU, it was nearly a direct match to the flight design. The second series of development testing began in December 2018 and ran through May 2019. Design updates have produced a more robust PPU that will meet all the mission requirements, including all EMI/EMC requirements and mechanical loads (shock and vibration). Development level TVAC testing was performed at NASA GRC across full protoflight temperatures, including survival temperatures, and across all Throttle Points (TLs) that the thruster would run. Protoflight baseplate temperatures are from -29°C to +55°C with a survival temperature range of -45°C to 76°C. EMI testing was also performed at NASA GRC. During EMI testing in Jan 2017, a handful of facility limitations were identified. These limitations were resolved and the PPU underwent EMI/EMC testing again in February of 2019. Overall, the EMI results were remarkable for a 7kW PPU. Shock testing was then performed at Delserro and random and sine vibe testing performed at Rockwell. Figure 13 shows the PPU on the vibration table at Rockwell.

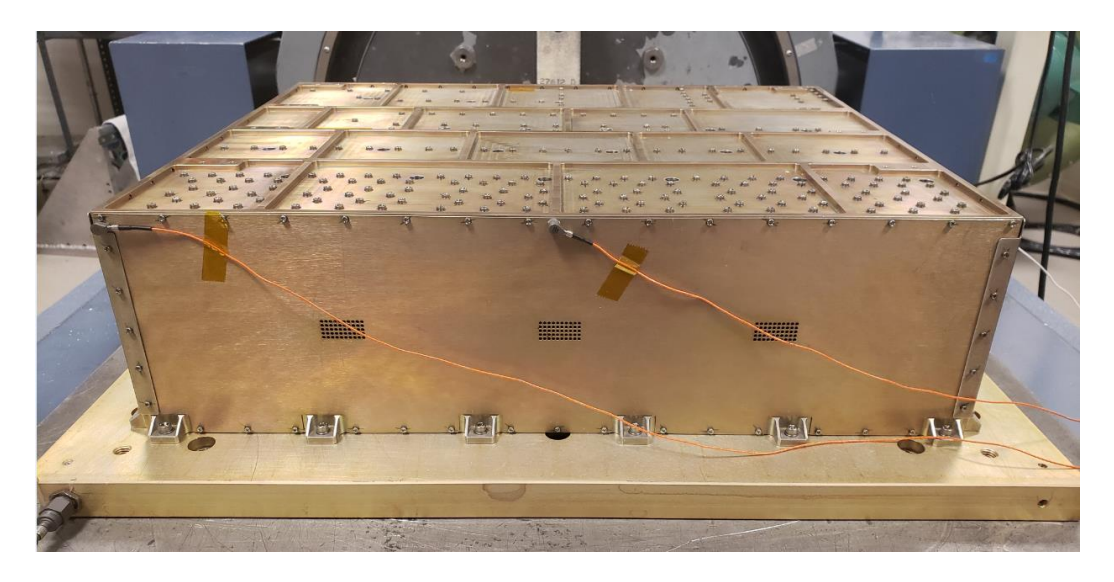


Fig. 13 Prototype PPU Vibration Testing.

Starting in August of 2018, a series of System Integration Tests (SITs) were successfully performed with the NEXT-C prototype hardware at NASA GRC. These tests involved the efforts of a multidisciplinary team of AR, NASA, APL, and ZIN Technologies personnel. The testing consisted of using the prototype PPU to power the development thruster (Dev-C) as a system, including some tests where the DART mission command software was utilized. The tests were focused on verifying that the components work properly together and provide the DART team with data for mission planning and spacecraft operations.

All three of the development SITs were performed at NASA GRC using the same test facilities. The prototype model thruster (Dev-C) was operated in VF-16. The Prototype PPU was operated in a dedicated vacuum facility (VF-14) to protect it from back-sputtered facility material and to allow for quicker problem resolution should the unit require atmospheric exposure for access. Commercial mass flow controllers were used to provide high-purity Xenon to the thruster and provided independent flow control over the expected flow rates to each of the three thruster propellant inputs: neutralizer, cathode, and main. DART's development environment revolves around the enhanced software in the loop simulator (SWIL) environment which enables flight software development and testing of Flight Software on Commercial Off-The-Shelf (COTS) machines. The SWIL provides an early, medium-fidelity test environment that can easily scale for extensive test regimes by allowing a developer to practically have a spacecraft on a laptop. A schematic and photograph of the apparatus are shown in Figs. 14 and 15, respectively.

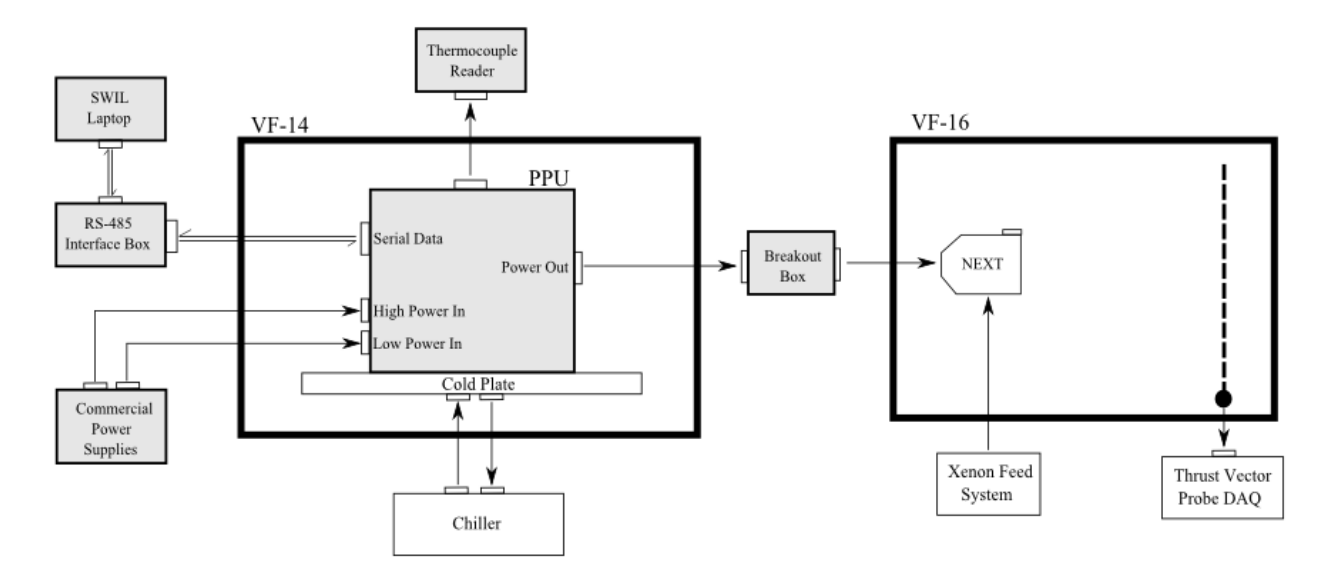


Fig. 14. Block diagram of the integration test facilities.

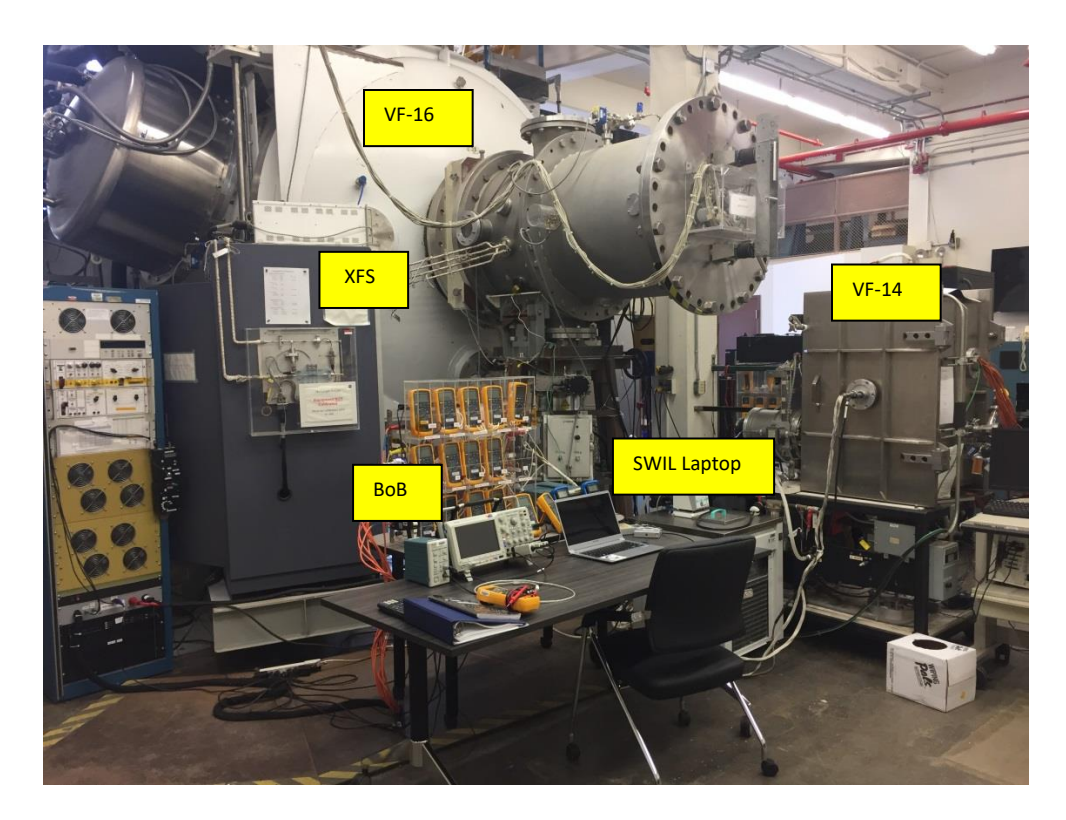
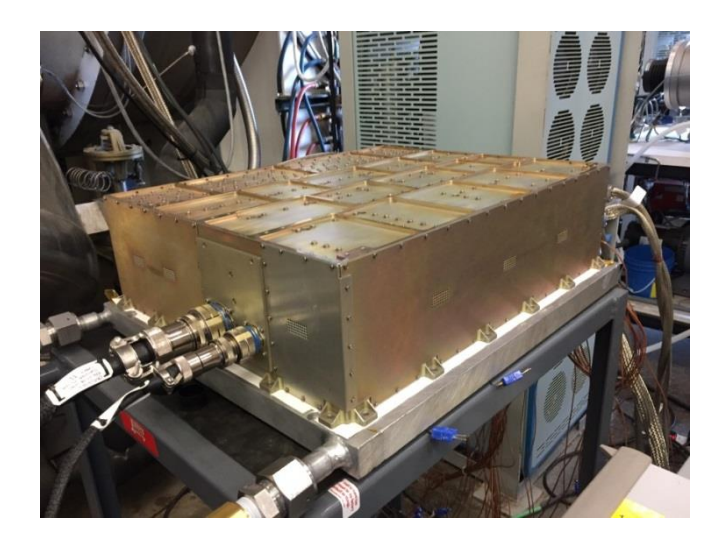


Fig. 15. Physical layout of the system integration test facilities.



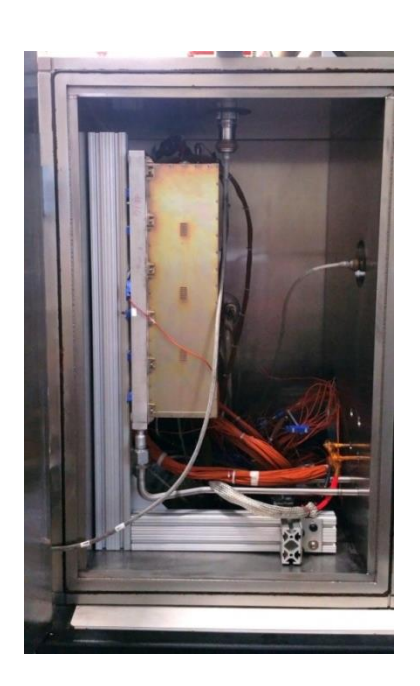


Fig. 16a and 16b. PPU mounted on the external cold plate and within VF-14.

The Preliminary SIT (PSIT) was performed in September 2018 for a quick evaluation of the interfaces and risk mitigation for the upcoming DART SIT. The DART SWIL code operated the PPU by commanding both individual power supplies and performing sequences (e.g. cathode conditioning, thruster start, throttle and operation with beam control) on the resistive load. A check out test was then performed using the Dev-C thruster at TL28. The tests were successful and identified some minor items to be corrected for the DART SIT.

The DART SIT was performed in October 2018. This test was focused on operating at the DART flight conditions plus high and low margins (flow rates and PPU input voltages). It used the next version of the DART flight software. The thruster and PPU performance data collected from this test provided the DART team with a good baseline for mission planning. The upgraded DART SWIL code operated the PPU and performed sequences (e.g. cathode conditioning, thruster start, throttle and operation with beam control) on the resistive load. This testing also included PPU fault detection capture and response, and simulated recycle events. The system was then reconfigured to operate the Dev-C thruster for a series of tests at the DART operating conditions (ETL2.7a, TL28 and TL29) at PPU temperatures ranging from -29°C to 55°C, PPU High Power Bus (HPB) input voltages from 80V to 125V and over a range of mass flow rates (nominal plus worst case low and high). All of the testing was successful.¹⁵

The third development SIT used the NEXT-C operating conditions and was performed in March 2019. The set up for this SIT was the same as the previous tests except the PPU was commanded by the Zin Technologies DCIU simulator system. This test operated the system over a wider range of Throttle Levels (TL05, TL09, TL12, TL22, TL29, TL32, and TL40) at the nominal NEXT-C mass flow rates. Tests were also performed at TL05 with the PPU baseplate at -29°C and TL05, TL37 and TL40 with the PPU baseplate at 55°C. System starts were performed at HPB voltages of 80V, 120V and 160Vand with the PPU at -29°C, 25°C and 55°C. The standard PPU fault conditions were all tested with the thruster as a load and the PPU performed as expected. The tests showed that, as expected, the thruster operation and performance was insensitive to the PPU operating conditions (HPB voltage or PPU temperature). Testing limitations of using long laboratory power cables were also investigated using both the original cables and shorter ones with larger wire diameters that were planned to be used on flight hardware SIT.

VIII. Flight Hardware Testing

Both the flight thruster and flight PPU successfully completed protoflight level testing to verify operation of each component as well as mitigate risk of anomalies during system testing of the flight hardware. This included multiple integrated system tests, including ones that direct simulated the mission operating parameters for the DART mission.

Flight Thruster testing was completed in January 2020 and included two segments: 1) Acceptance Testing (Performance Acceptance Testing, vibration, TVAC and Functional tests) and 2) System Integration Testing as shown in Fig. 17. All of these tests were performed at NASA GRC. Summary level performance data is provided below, with more detailed information to be provided in a future, to be published paper.

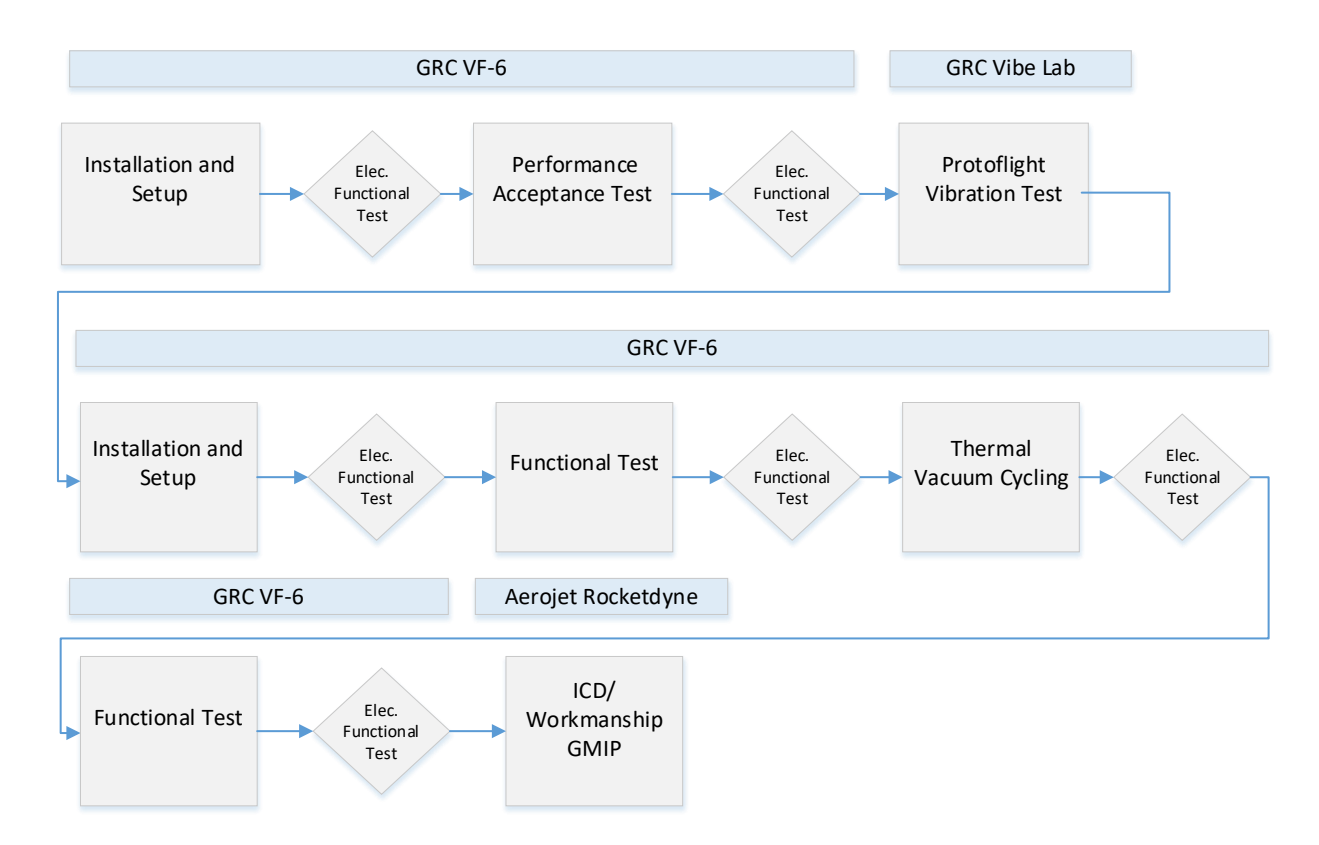


Fig. 17 Flight Thruster Testing Campaign.

Table 3. Flight Thruster Hot Fire Test Points during Performance Acceptance Testing.

V V _{pbs} ,	1800	1567	1396	1179	1021	936	850	679	650	400	300	275
3.52	TL40	TL39	TL38	TL37								
3.10	TL36	TL35	TL34	TL33								
2.70	TI32	TL31	TL30	TL29	TL28	ETL2.7A						
2.35	TL27	TL26	TL25	TL24	TL23							
2.00	TL22	TL21	TL20	TL19	TL18							
1.60	TL17	TL16	TL15	TL14	TL13							
1.20	TL12	TL11	TL10	TL09	TL08	TL07	TL06	TL05	TL04	TL03	TL02	
1.00												TL01

During all the performance testing shown in Table 3, a suite of plasma diagnostics were employed to measure the characteristics of the ion beam downstream of the thruster. The plasma diagnostics suite is comprised of a near field Faraday probe located 4.5 cm downstream of the accelerator grid, a mid-field Faraday probe located 82 cm downstream of the accelerator grid and a far field Faraday probe located 2.7 m downstream of the accelerator grid. In addition to these three Faraday probes, a single ExB probe was located on the mid-field probe suite and data were 82 cm downstream of the accelerator grid. The mid-and far field Faraday probes, and this ExB probe rotated about the center of curvature for the ion optics and the near field probe moved at a constant axial position. The purpose for these probes is to correct the computed thrust for slight variation in the ion beam divergence and composition. Specifically the far-field probe at 2.7 meters is used to correct the thrust for the beam divergence and the ExB probe and the near-field probe are used to correct for the fraction of double to single ions within the ion beam. In addition to the four plasma probes associated with the experimental apparatus, to gain more insight on the performance of the proto-flight thruster, a thrust vector probe was installed and used during all the testing conducted. This thrust vector probe is similar in design to the probe developed by JPL and used to measure the thrust vector for the NSTAR thruster. The thrust vector probe has 16 vertical and horizontal rods, an outside dimension of 2.54 m and the array was located 12.4 m downstream of the thruster. Based upon the size and location of the probe, the acceptance half angle is ~13 degrees.

As indicated on Fig. 17, the test campaign for the flight thruster involved an initial Performance Assessment Test (PaT) in which the baseline performance of the thruster was measured, as shown in Table 4. At the completion of the PaT, the thruster was removed from the vacuum facility and transported to the Structural Dynamics Laboratory at NASA GRC for vibration testing, as shown in Figure 18. The thruster was subject to a proto-flight random vibration test. For each axis perpendicular to the thrust axis, the thruster was subject to a vibration level of 15.9 G_{rms} and in the thrust axis direction, the thruster was subjected to a level of 14.7 G_{rms}. A comparison of the sine sweep profiles taken before and after the vibration testing showed negligible changes in the fundamental frequencies associated with the thruster. At the completion of the successful vibration test, the thruster and a thermal shroud were installed in the VF6 facility, as shown in Figures 19 and 20, and an abbreviated function test (FuT) was performed to verify that the performance of the thruster had not changed due to the vibration testing. For this FuT, the operating points were limited to those required by the DART mission. These data were then compared to those obtained during the initial PaT to verify that there were indeed no changes to the performance. Next the thruster was subjected to a thermal vacuum test in which it was subject to three cycles from -110°C to 190°C. The hot temperature was limited by a test setup that excessively heated the external thruster cabling. Despite this limitation, the hot temperature demonstrated was still greater than that required by the DART mission. Lastly, as the completion of the TVAC test, the thruster was again subjected to a FuT performance test at the DART operating conditions and again verified the performance of the thruster was unaffected. A comparison of these data was performed to show any changes that may have been caused by either vibration or TVAC testing. Table 5 contains the performance data computed for TL29, TL28, ETL2.7A and TL05. Contained on the table are the total input power for the thruster, the computed thrust and specific impulse and efficiencies. In addition, for each parameter the average of the three measurements and the coefficient of variation are presented as a measure of the variability for the three measurements. Lastly, for the DART throttle levels of TL29, TL28 and ETL2.7A, the requirement value is provided and for TL05 a reference value obtained from previous family testing is provided. Reviewing the table shows that for the DART conditions, the covariance (CoV) for the input power is less than 0.20% showing very good agreement between the values. Similarly, for the thrust, specific impulse and efficiency, the highest CoV is 1.4% for the efficiency which shows good agreement between the tests. For the TL05 data, the highest CoV is less than 1% which again shows very good agreement between the three tests at this operating condition. This observation suggests that neither the vibration testing of the TVAC testing affected the operation of the thruster. It should be noted that the slight out of specification values for the thruster efficiency are due to insufficient margin being applied to the values and when they were established and do not indicate an issue with the thruster. Additional thruster performance data taken during flight thruster testing to be provided in a future, [to be published] paper.

Table 4. Flight Thruster Hot Fire Performance during Performance Acceptance Testing.

Throttle Level	TL40	TL37	TL29	TL28	ETL2.7A	TL09	TL05					
Thruster Perfo	Thruster Performance (Performance Acceptance Test)											
P _{tot} , kW	6.83	4.69	3.62	3.21	2.99	1.70	1.12					
T, mN	233.7	192.1	146.7	137.5	131.7	63.8	48.9					
l _{sp} , s	4148	3410	3365	3153	3055	3190	2443					
3	69.5%	68.4%	66.9%	66.2%	66.0%	58.7%	52.3%					

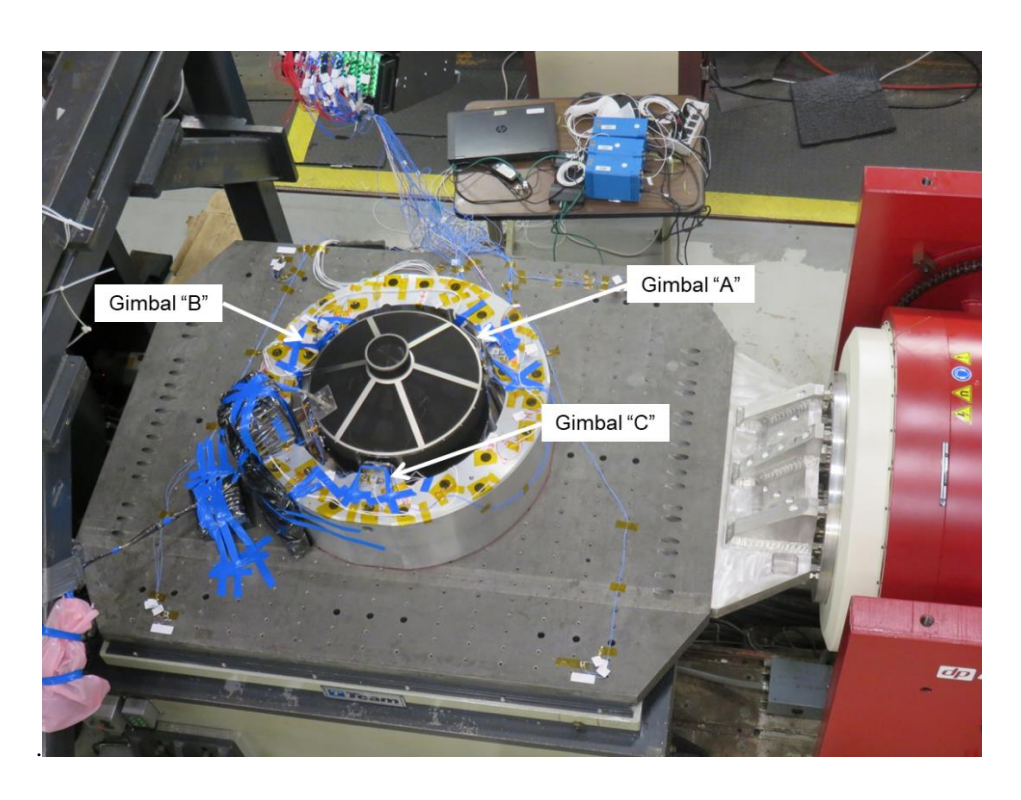


Fig. 18 Flight Thruster Undergoing Vibration Testing



Fig. 19 Flight thruster installed in the thermal shroud in NASA GRC's VF6.

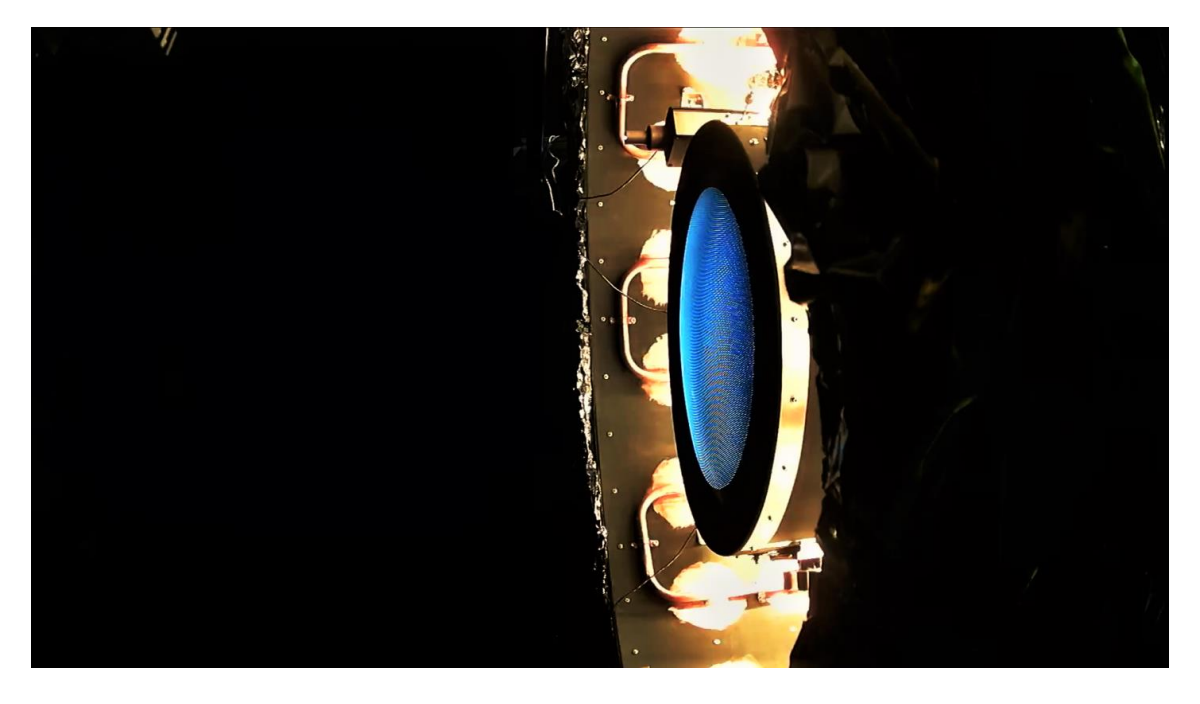


Fig. 20 Flight thruster operating during the protoflight level thermal vacuum testing.

Table 5 Comparison of initial thruster performance to that measured after vibration and TVAC testing

TL:	TL29				TL28				ETL2.7A				TL05			
J _b , V _b :		2.70 A, 1179 V			2.70 A, 1021 V			2.70 A, 936 V				1.20 A, 679 V				
Perf.	PaT	FuT	FuT	Req	PaT	FuT	FuT	Req	PaT	FuT	FuT	Req	PaT	FuT	FuT	Ref
P _{input} , kW	3.62	3.63	3.63	≤ 3.640	3.21	3.21	3.22	≤ 3.225	2.99	2.99	2.99	N/A	1.12	1.13	1.13	1.152
	Ave=	3.627	CoV=	0.20%	Ave=	3.213	CoV=	0.11%	Ave=	2.991	CoV=	0.10%	Ave=	1.127	CoV=	0.67%
T, mN	146.7	145.6	147.8	≥ 140	137.5	136.0	135.8	≥ 130	131.7	130.3	130.1	N/A	48.9	48.8	48.9	49
	Ave=	146.7	CoV=	0.73%	Ave=	136.4	CoV=	0.68%	Ave=	130.7	CoV=	0.68%	Ave=	48.9	CoV=	0.02%
I _{sp} , s	3365	3339	3338	≥ 3206	3153	3118	3114	≥ 2982	3055	3022	3017	N/A	2443	2443	2443	2455
	Ave=	3347	CoV=	0.46%	Ave=	3128	CoV=	0.69%	Ave=	3031	CoV=	0.69%	Ave=	2443	CoV=	0.02%
ε	0.669	0.657	0.656	≥ 0.66	0.662	0.647	0.645	≥ 0.65	0.660	0.646	0.643	N/A	0.523	0.519	0.516	0.51
	Ave=	0.66	CoV=	0.73%	Ave=	0.65	CoV=	1.40%	Ave=	0.65	CoV=	1.42%	Ave=	0.52	CoV=	0.65%

Flight PPU testing was successfully completed in late 2019 and included Calibration, extensive Performance Testing, EMI/EMC Testing, Random and Sine Vibration, TVAC, and 300 hour burn-in testing. An abbreviated Performance test, called "Functional Test" was performed as an entrance and exit to each critical environmental test.

The Calibration and Performance Test were the last "open box" tests for the PPU. The Calibration test characterized the PPU voltage and current outputs as a response to the digital DC-DC converter set point values. It also provided a temperature corrected telemetry correction curve to properly calibrate digital PPU flight telemetry relative to PPU voltage and current outputs. This calibration curve was then provided to the DART team and integrated into the flight DCIU software and demonstrated during the flight System Integration Test described later in this paper.

Because of the specified use of the first flight PPU on the DART mission, it was determined that the flight PPU would follow the "test like you fly" (TLYF) approach and would be tested to specific DART mission requirements. This meant a smaller subset of input voltages as well as output throttle points relative to the capability of the design as demonstrated on the prototype unit. Also, the environmental tests (vibration and TVAC) were specific to mission requirements, but remained at mission protoflight levels. Figures 21 - 25 show the flight PPU test setups along with summary level PPU efficiency data taken.



Fig. 21 Flight PPU Calibration and Performance Testing

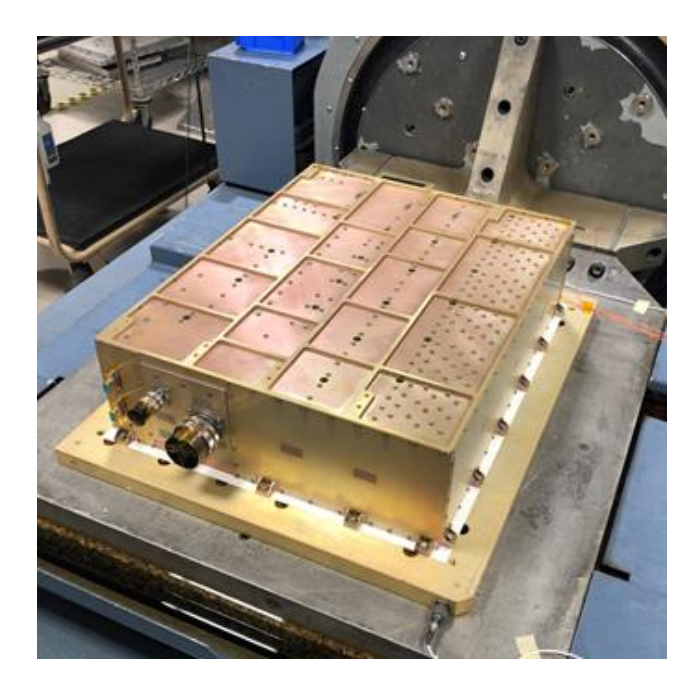


Fig. 22 Flight PPU Random and Sine Vibration Testing

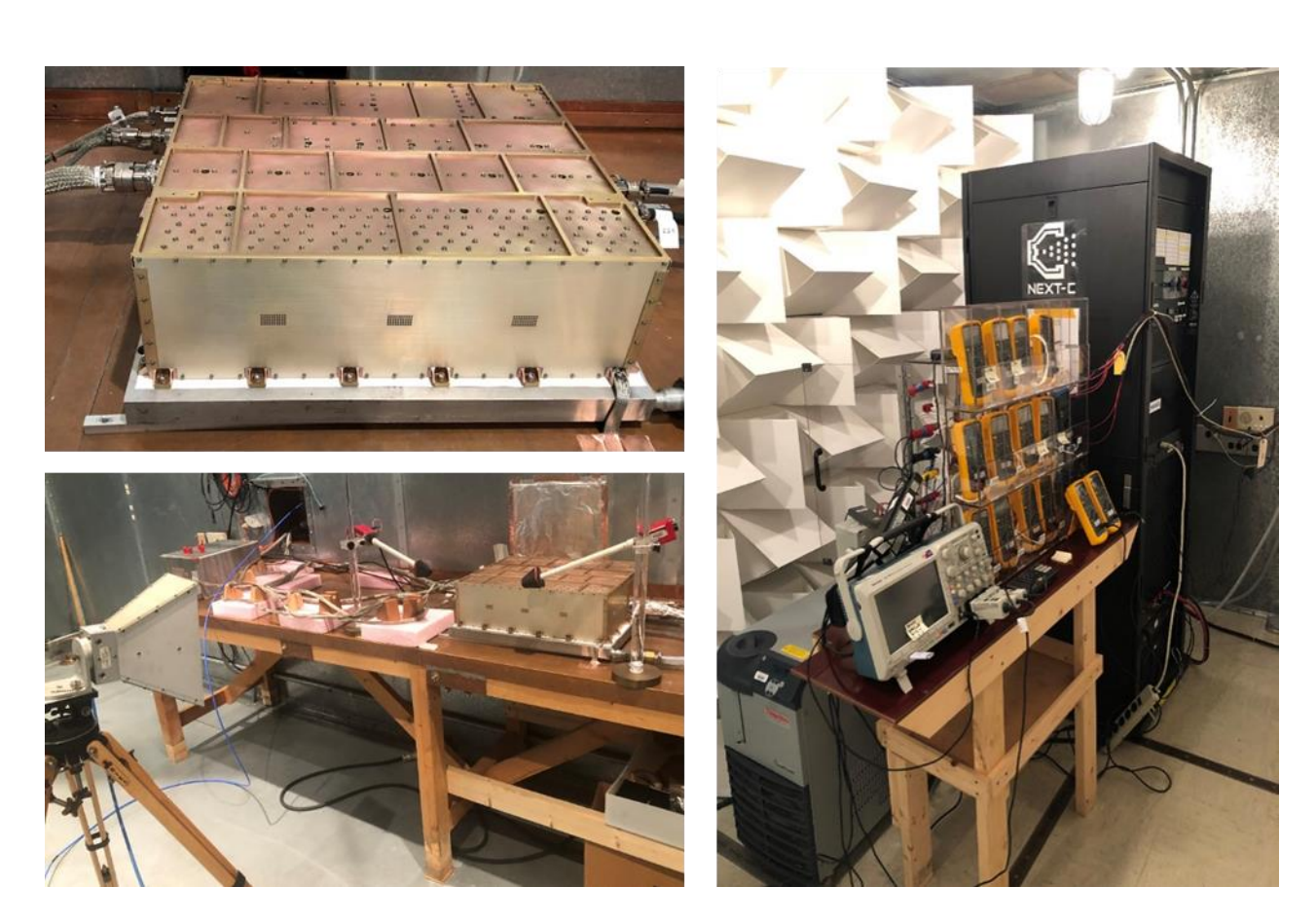
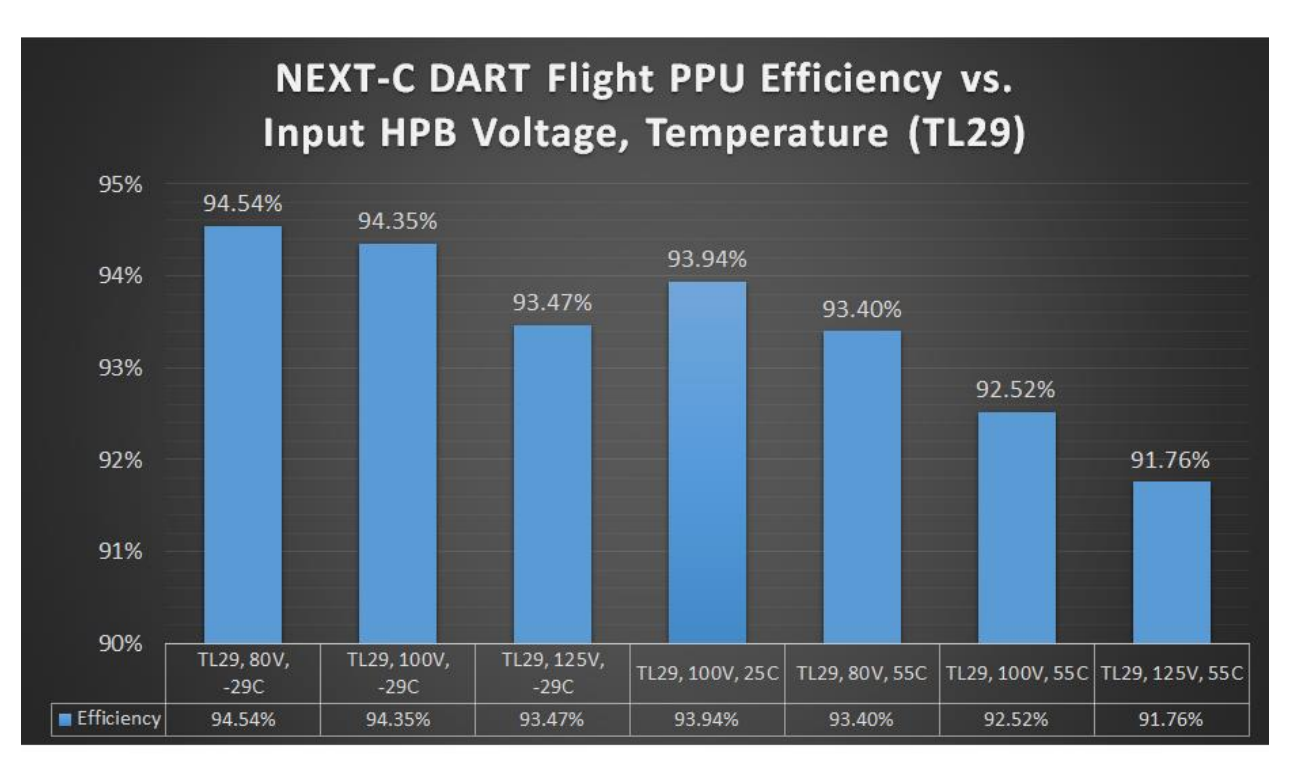


Fig. 23 Flight PPU EMI Testing



Fig. 24 Flight PPU TVAC Testing



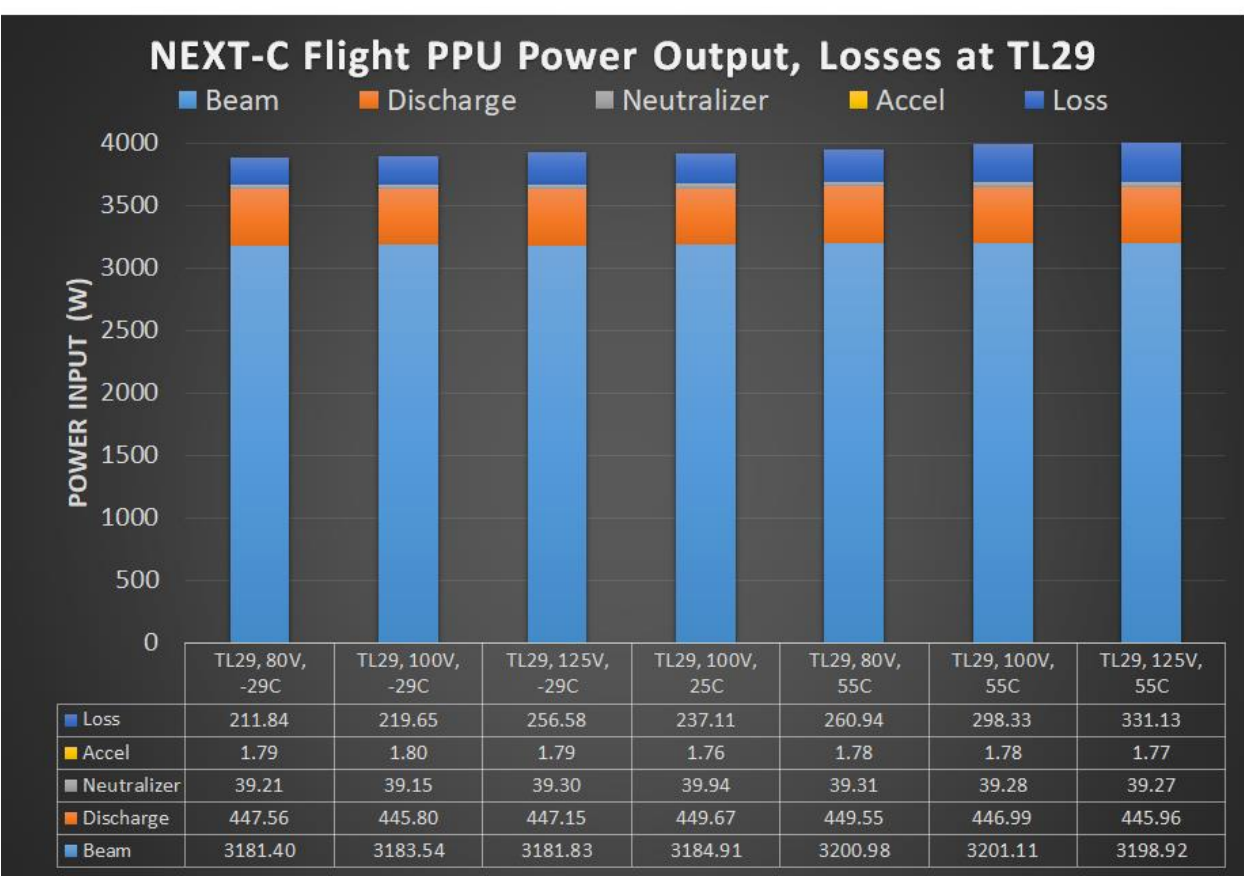


Fig. 25 Flight PPU Input Power, Output Power, and Efficiency Data Operating the Flight Thruster at TL29 as a Function of Input Voltage and Temperature.

In January of 2020, System Integration Testing was successfully performed with the flight hardware at NASA GRC. This SIT contained all of the DART flight hardware except the Xenon flow system, which was simulated. The test consisted of 3 major segments. For the first segment the PPU operated on a resistive load by the DART DCIU Simulator (DDS) utilizing the flight software. These tests verified proper operation of the DDS and PPU and tested conditions/faults/limits that were risky to initially perform with the flight thruster. Since the thruster had just completed acceptance testing, the Cathode Conditioning and Thruster Bakeout sequences were also verified using the resistive load. The second segment of tests were designed to be as close as to TLYF as possible. Testing was performed at ETL2.7a, TL28 and TL29, at the expected DART flow rates, and at the expected flight PPU baseplate temperature. The data from this test provided the DART flight team with the expected PPU and thruster performance data for mission planning and spacecraft operations. The third segment of testing involved performing 4 PPU TVAC cycles with the thruster as a load and different thruster operating conditions. The flight SIT tests were also used to verify several of the NEXT-C program System Requirements.

A schematic of the test setup is shown in Fig. 26. The flight thruster was operated in VF-6 and remained under vacuum following FuT2. Commercial mass flow controllers were used to simulate the flight feed system and provide high-purity Xenon to the thruster and provided independent flow control to each of the three thruster propellant inputs. The same thruster thermal shroud system used in the thruster TVAC testing was used, as shown in Figure 27. The PPU was set up on a cold plate in an adjacent vacuum chamber (VF-18). The PPU received power from two supplies: a low voltage, 22-24V supply and a high voltage 80-125V supply. The PPU provided two output lines to the thruster, one for the neutralizer and one for the discharge. Control and telemetry for the PPU was provided by the DDS.

The system was operated at the three DART throttle levels. At each throttle level, the PPU's low and high voltage inputs were swept through their operating ranges. This was both to ensure the PPU could operate over its full required range and to exercise the PPU beam module Pulse Width Modulation (PWM) to phase shift mode transition functionality. Collected data included PPU telemetry, verification of telemetry from the PPU breakout box multimeters, thruster voltages, vacuum chamber pressure, neutralizer voltage and current ripple, neutralizer spotplume mode transition flowrate, electron back streaming voltage, and Faraday and ExB probe data. Additionally, recycles were forced at each throttle point to ensure the system could recover from recycle events. The system successfully demonstrated recovery from forced recycle events, along with naturally occurring ones experienced during operation. At specific throttle levels, the number of active PPU beam modules was reduced by one to demonstrate the ability to operate at these levels in the event of a single module failure. The test spanned several days, and at the conclusion of each test day the system's operation was terminated by triggering one of several limits meant to force safe shutdown of the PPU in the event of limit violation.

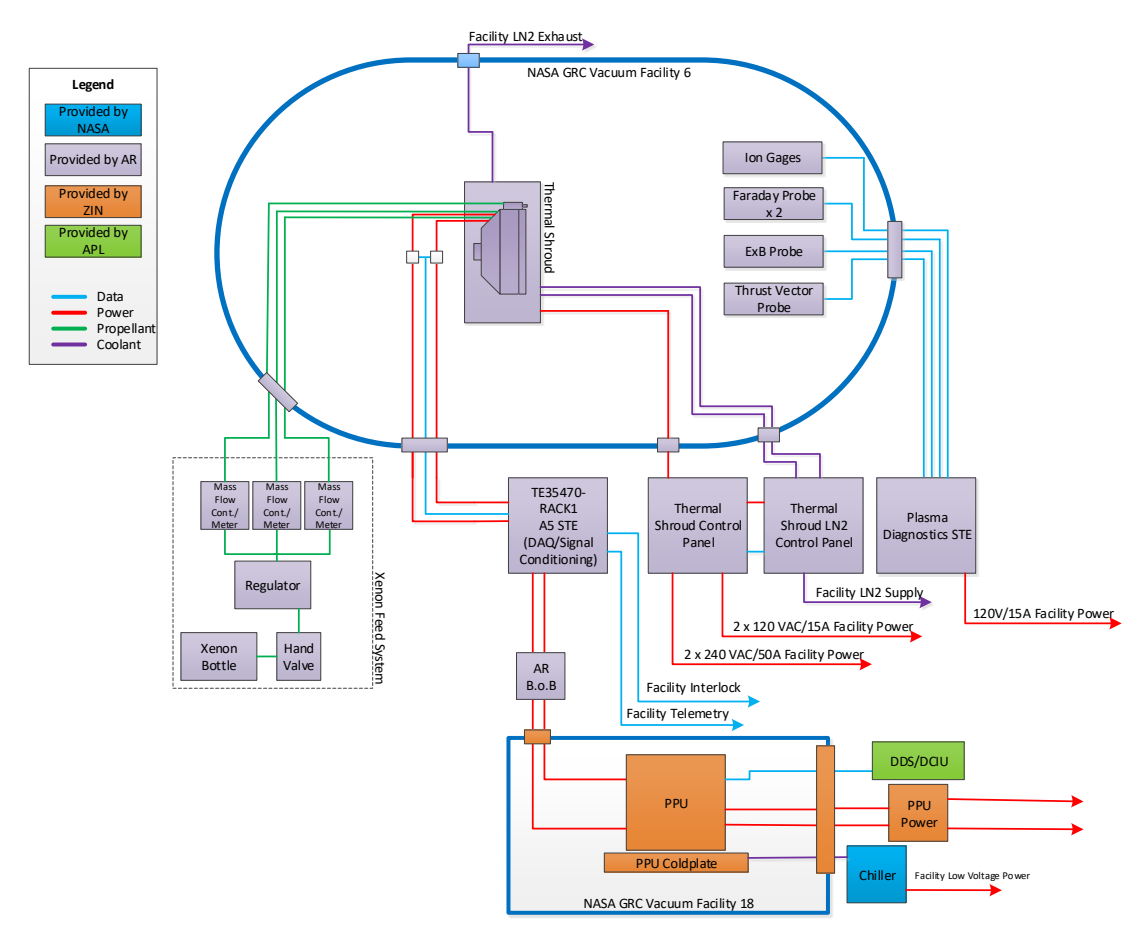


Fig. 26. Block diagram of the flight hardware SIT equipment

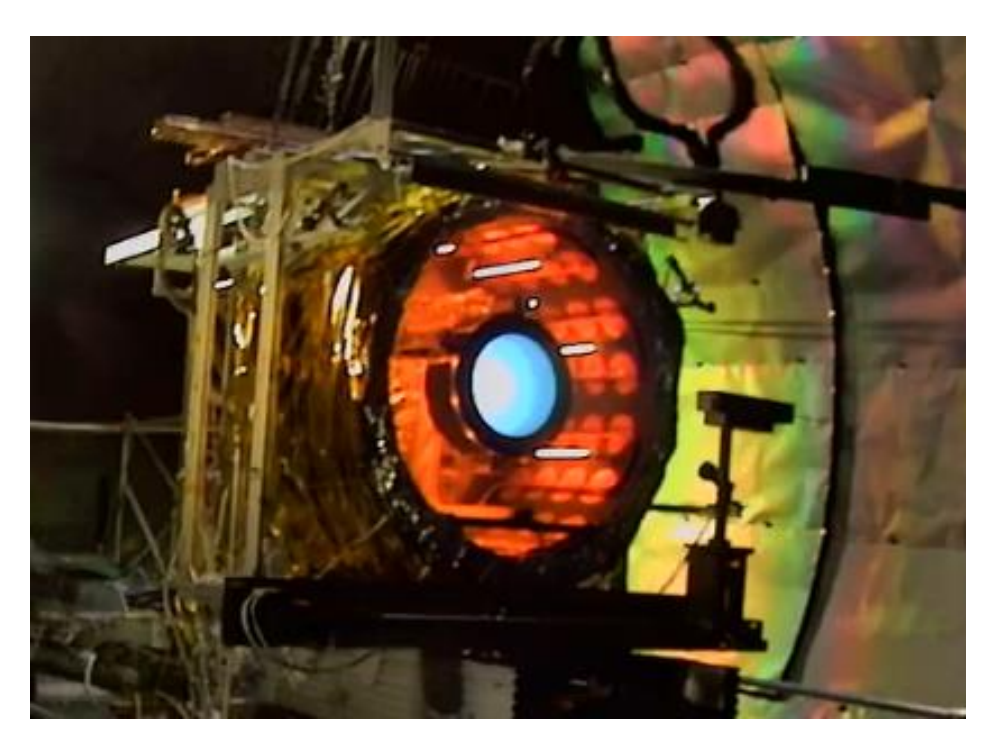


Fig. 27 Flight thruster operating during hot cycle during SIT

The thruster performance data for the TLYF segment is shown in Table 6. The table shows the total power (Ptot), thrust (T) and specific impulse (Isp) for the three test sequences (the Pa T, the Fu 2 and SIT) at two throttle set points (TL 28 and TL 29). The voltages noted in the table (SIT columns) are the HPB input voltages to the PPU. Note that the flow rates for the DART test were higher than NEXT-C ones used for the PAT and FuT2 tests so the Isp is expected to be lower for the SIT. The nominal flow rates for DART are: main is 37.73 sccm, Discharge Cathode is 4.20 sccm and the Neutralizer Cathode is 5.46 sccm. The results show that the thruster performance was in family with the PAT and FuT data. The PPU data from the TLYF segment is shown in Fig. 28. This data is consistent with the PPU ATP data, as expected.

Table 6. Thruster performance from SIT compared to ATP data

		P _{tot} (W	()		T (mN)		I _{sp} (s)			
Throttle Level	PAT	FuT 2	SIT	PAT	FuT 2	SIT	PAT	FuT 2	SIT	
TL28	3203	3207	80V: 3203 100V: 3201 125V: 3205	137.9	136.2	136.06 (125V)	3162	3123	2986 (125V)	
TL29	3608	3622	80V: 3612 100V: 3614 125V: 3615	147.2	146.0	145.61 (125V)	3375	3347	3201 (125V)	

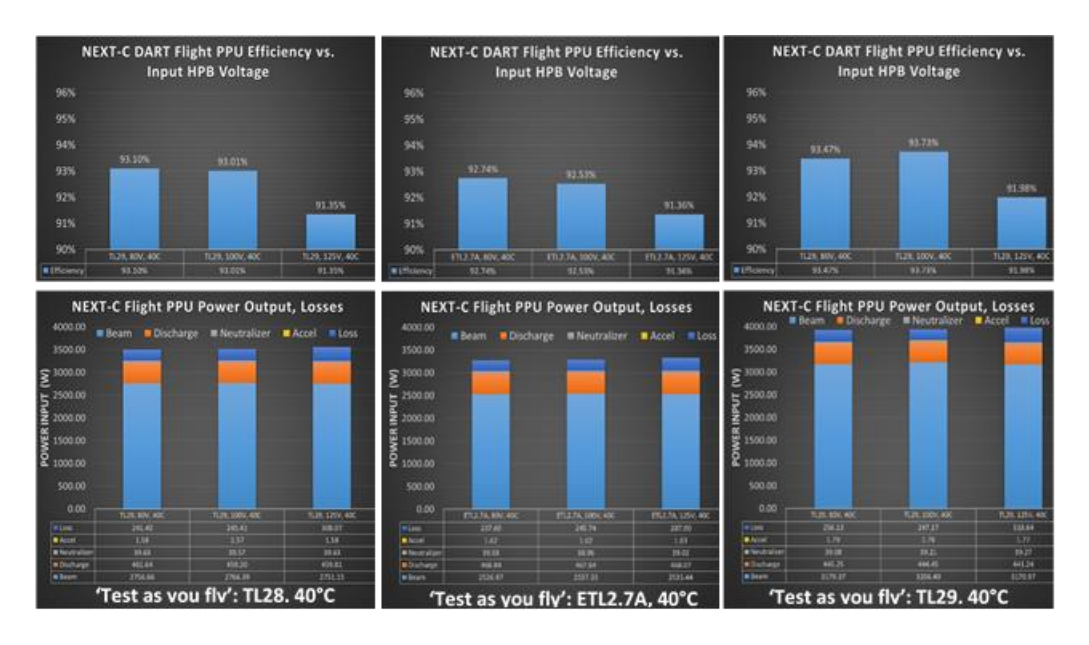


Fig. 28 PPU performance from SIT TLYF segment.

The third segment of SIT performed 4 PPU TVAC cycles with different thruster operating conditions (TL28 with high flows, TL28 with low flows, ETL2.7a with nominal flows and a hot thruster, and TL29 with nominal flows and a cold thruster). The operating conditions were selected to envelop the expected DART flight conditions as much as possible. A cold thruster ignition was performed each morning of the 4 PPU cycle tests (one per day) to test worst case starting conditions. A program requirement was to perform a total of 10 PPU TVAC cycles. Six were performed

in the PPU ATP with the resistive load and 4 were performed in the SIT with the thruster as a load. The thruster performance was again insensitive to the PPU operating conditions (HPB voltage or PPU temperature) as expected. There were expected changes in the PPU loading due to the changes in the thruster operating conditions (flow rates and temperature) but all of them were small. This completed the test campaigns for the flight hardware (except for standard functional tests).

IX. Conclusions

The NEXT ion propulsion system has been shown to be ideally suited for a wide range of NASA robotic science missions as well as several national and commercial orbit raising missions. The NEXT-C program has completed all phases of the project, including development hardware build and testing, demonstrating the full range of NEXT-C operating parameters, Critical Design Review, ground test equipment validation, fabrication of flight hardware, protoflight level acceptance testing and delivery to the first flight mission spacecraft. Flight hardware testing included both component level testing of the flight PPU and thruster, culminating in a System level hot fire test that demonstrated the flight controls and operating parameters planned to be utilized on the DART mission. The flight hardware testing was successfully completed in early 2020, and the first set of flight hardware has been delivered to JHU/APL in support of the DART mission.

X. Acknowledgments

The NEXT-C program team would like to thank the Planetary Science Division of the Science Mission Directorate, NASA Headquarters, for their continued support of the work discussed in this paper and all the NEXT-C reviewers, technical consultants and team members at Aerojet Rocketdyne, ZIN Technologies, and NASA who have contributed to the success of the program.

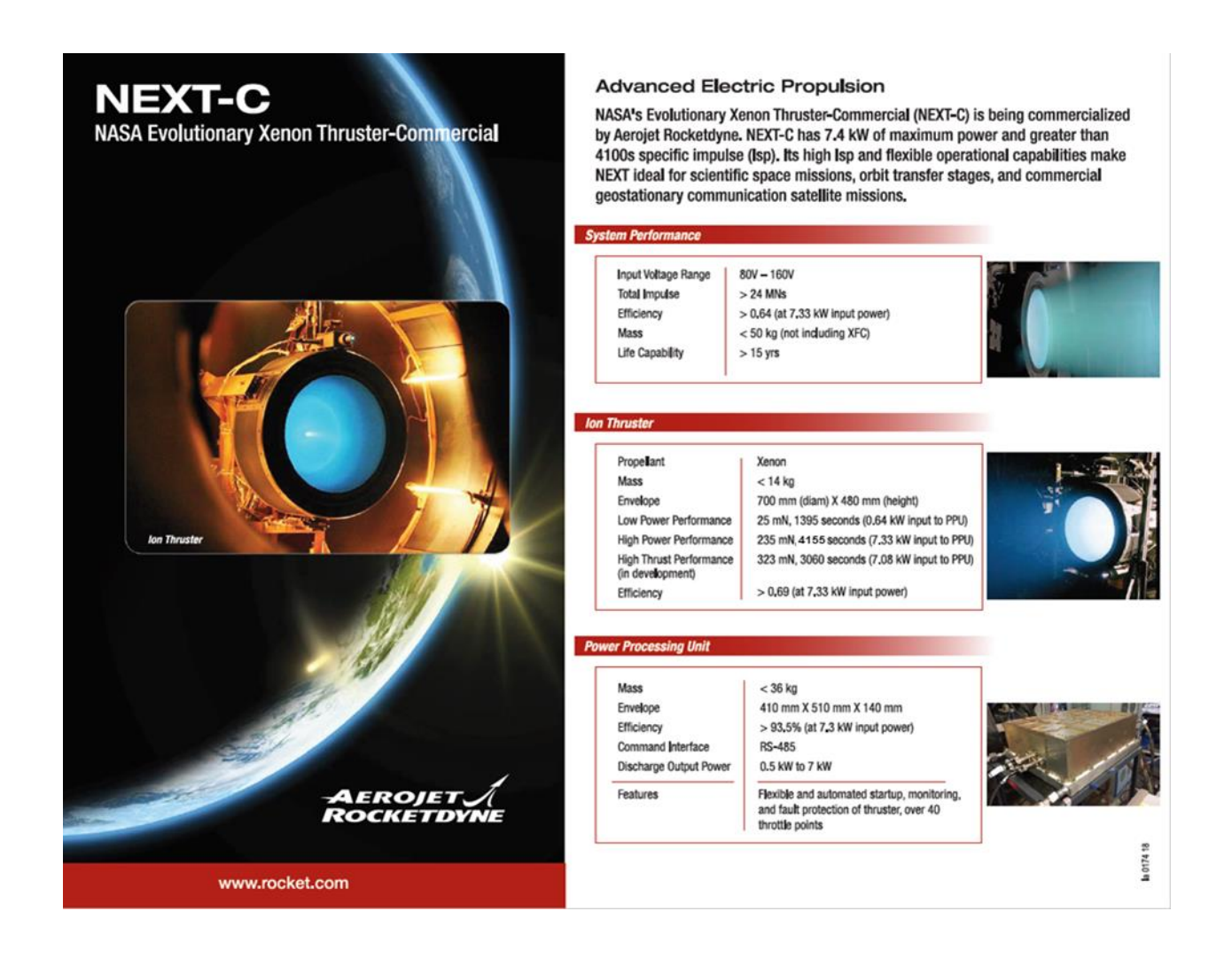


Fig. 29 NEXT-C Product Data Sheet.

XI. References

- [1] Leary, J., Strain, R., Lorenz, R. and Waite, J.; Titan Explorer: Flagship Mission Study; The Johns Hopkins Applied Physics Laboratory, Jan. 2008.
- [2] Benson, S., Lo, A., and Glassman, T.; "Solar Electric Propulsion for the New Worlds Observer Terrestrial Exoplanet Mission," 45th Joint Propulsion Conference, Denver, CO, 2009, AIAA-2009-5094.
- [3] Lock, R., et al., "Mars Sample Return Orbiter Concepts using Solar Electric Propulsion for the post-Mars 2020 Decade, IEEE Aerospace Conference, Big Sky, Montana, March 2014.
- [4] Reed, C., Cheng, "Asteroid Impact Deflection Assessment: Double Asteroid Redirection Test," IAC-16, A3,4,10,x32340, International Astronautical Federation, Sept. 2016.
- [5] Polk, J., et al, "Demonstration of the NSTAR Ion Propulsion System on the Deep Space One Mission," IEPC-01-075, 27th Int. Electric Propulsion Conference, Pasadena, CA, Oct. 2001.
- [6] Hoskins, W. A., et al., "NEXT Ion Propulsion System Production Readiness," AIAA 2007-5856, 43rd Joint Propulsion Conference, Cincinnati, OH July 2007.
- [7] Patterson, M., and Benson, S., "NEXT Ion Propulsion System Development Status and Performance," AIAA 2007-5199, 43rd Joint Propulsion Conference, Cincinnati, OH July 2007.
- [8] Shastry, R., et al., "Status of NASA's Evolutionary Xenon Thruster (NEXT) Long-Duration Test as of 50,000 h and 900kg Throughput," IEPC-2013-121, 33rd Int. Electric Propulsion Conference, Washington, D.C., Oct 2013.

- [9] Shastry, Rohit, Daniel A. Herman, George C. Soulas and Michael J. Patterson "End-of-test Performance and Wear Characterization of NASA's Evolutionary Xenon Thruster (NEXT) Long Duration Test", AIAA-2014-3617 50th AIAA/ASME/SAE/ASEE Joint Propulsion Conference, Cleveland, OH, July 28-30, 2014
- [10] Benson, S., Patterson, M., and Snyder, J., "NEXT Ion Propulsion System Progress Towards Technology Readiness," AIAA 2008-5285, 44th Joint Propulsion Conference, Hartford, CT, July 2008.
- [11] Bruno V. Sarli, Martin T. Ozimeky, Justin A. Atchisonz, Jacob A. Englander, and Brent W. Barbee, "NASA Double Asteroid Redirection Test (DART) Trajectory Validation And Robustness", AAS 17-206, 27th AAS/AIAA Space Flight Mechanics Meeting, San Antonio, TX, February 5-9, 2017.
- [12] Soulas, G., "The Impact of Back-sputtered Carbon on the Accelerator Grid Wear Rates of the NEXT and NSTAR Ion Thrusters, IEPC-2013-157, 33rd Int. Electric Propulsion Conference, Washington D.C., Oct 2013.
- [13] Chaplin, V. H., Polk, J. E., Katz, I., Anderson, J. R., Williams, G. J., Soulas, G. C., and Yim, J. T., "3d simulations of ion thruster accelerator grid erosion accounting for charge exchange ion space charge," 54th AIAA/SAE/ASEE Joint Propulsion Conference, 2018, AIAA-2018-4812.
- [14] Polk, J.E, Chaplin, V., Yim, J., Soulas, G. Williams, G., and Shastry, R., "Modeling Ion Optics Erosion in the NEXT Ion Thruster Using the CEX2D and CEX3D Codes," 36th International Electric Propulsion Conference, 2019, Paper IEPC-2019-907.
- [15] Thomas, R., Aulisio, M., Badger, A., Heistrand, D., Thompson, D., Liang, R., John, J., Goodfellow, K., and Bontempo, J., "NEXT Single String Integration Tests in Support of the Double Asteroid Redirection Test Mission," IEPC-2019-853, 36th Int. Electric Propulsion Conference, Vienna, Austria, Sept 2019.
- [16] Bontempo, J., Brigeman, A., Fain H., Gonzalez, M., Pinero, L., Aulisio, M., Birchenough, A., Fischer, J., Ferraiuolo, B., "The NEXT-C Power Processing Unit: Lessons Learned from the Design, Build, and Test of the NEXT-C PPU for APL's DART Mission," AIAA-2020-TBD, 2020 AIAA Propulsion and Energy Forum, August 24-26, 2020.
- [17] Fisher, J., Ferriauolo, B., Monheiser, J., Barlog, C., Allen, M., Myers, R., Hoskins, A., Bontempo, J., Nazario, M., Shastry, R., Soulas, G., Aulisio, M., "NEXT-C Flight Ion Propulsion System Development Status", 35th International Electric Propulsion Conference, Atlanta, GA, 2017, Paper IEPC-2017-218.

32